On the Formulation of Coupled Thermoplastic Problems with Phase-change

C. AGELET DE SARACIBAR[†], M. CERVERA[‡] & M. CHIUMENTI[‖]
ETS Ingenieros de Caminos, Canales y Puertos
International Center for Numerical Methods in Engineering
Edificio C1, Campus Norte, UPC, Gran Capitán s/n, 08034 Barcelona, Spain

SUMMARY

This paper deals with a numerical formulation for coupled thermoplastic problems including phase-change phenomena. The final goal is to get an accurate, efficient and robust numerical model, allowing the numerical simulation of solidification processes in the metal casting industry. Some of the current issues addressed in the paper are the following. A fractional step method arising from an operator split of the governing differential equations has been used to solve the nonlinear coupled system of equations, leading to a staggered product formula solution algorithm. Nonlinear stability issues are discussed and isentropic and isothermal operator splits are formulated. Within the isentropic split, a strong operator split design constraint is introduced, by requiring that the elastic and plastic entropy, as well as the phase-change induced elastic entropy due to the latent heat, remain fixed in the mechanical problem. The formulation of the model has been consistently derived within a thermodynamic framework. The constitutive behavior has been defined by a thermoelastoplastic free energy function, including a thermal multiphase change contribution. Plastic response has been modeled by a J2 temperature dependent model, including plastic hardening and thermal softening. A pressure and mean gas temperature dependent thermal contact model has been used. Additionally, a gap dependent thermal model has been used to take into account surface heat transfer phenomena when the two bodies lose contact. Heat generation due to frictional dissipation has been also included. The numerical model has been implemented into the computational Finite Element code COMET developed by the authors. A numerical assessment of the isentropic and isothermal operator splits, regarding the nonlinear stability behavior, has been performed for weakly and strongly coupled thermomechanical problems. Numerical simulations of solidification processes show the performance of the computational model developed.

1. INTRODUCTION

Numerical solution of coupled problems using staggered algorithms, is an efficient procedure in which the original problem is partitioned into several smaller sub-problems which are solved sequentially. For thermomechanical problems the standard approach exploits a natural partitioning of the problem in a mechanical phase, with the temperature held constant, followed by a thermal phase at fixed configuration. As noted in SIMO & MIEHE [1991] this class of staggered algorithms falls within the class of product formula algorithms arising from an operator split of the governing evolution equations into an isothermal step followed by a heat-conduction step at fixed configuration. A recent analysis in ARMERO & SIMO [1992A,1992B,1993] shows that this isothermal split does not preserve the contractivity property of the coupled problem of (nonlinear) thermoelasticity, leading to staggered schemes that are at best only conditionally stables. ARMERO & SIMO [1992A,1992B,1993] proposed an alternative operator split, henceforth referred to as the isentropic split, whereby the problem is partitioned into an isentropic mechanical phase,

---

[†] Professor of Continuum Mechanics, [‡] Professor of Structural Mechanics, [‖] Graduate Research Assistant.

with total entropy held constant, followed by a thermal phase at fixed configuration. It was shown by ARMERO & SIMO [1992A,1992B,1993] that such operator split leads to an unconditionally stable staggered algorithm, which preserves the crucial properties of the coupled problem.

The remaining of the paper is as follows. Section 2 deals with the formulation of the local governing equations of the coupled thermoplastic problem, consistently derived within a thermodynamic framework. An additive split of the strain tensor and the entropy has been assumed. A particular J2-thermoplastic constitutive model, with temperature dependent material properties, has been considered. Latent heat associated to the phase-change phenomena has been incorporated to the thermal contribution of the free energy function. Plastic response has been modeled by a J2 temperature dependent model including nonlinear hardening due to plastic deformation and a thermal linear softening behavior. A brief summary of the thermomechanical frictional contact model is included. This Section ends with the variational formulation of the coupled problem.

In Section 3, fractional step methods arising from an operator split of the governing differential equations are considered. Isentropic and isothermal splits are introduced and nonlinear stability issues linked to the splits are adressed. A key point of the formulation of the isentropic split is the set up of the additional design constraints to define the mechanical problem. These additional constraints motivate the definition of the sets of variables and nonlinear operators introduced in the present formulation. Within the time discrete setting, the additive operator splits lead to a product formula algorithm and to a staggered solution scheme of the coupled problem. Finally, the time discrete variational formulation of the coupled problem, using isentropic and isothermal splits, is introduced.

Section 4 deals with a numerical assessment of the accuracy and stability properties of the operator splits for weakly and strongly coupled thermomechanical problems and with the numerical simulation of solidification processes. Numerical results are compared with available experimetal data.

Some concluding remarks are drawn in Section 5. For convenience, a step-by-step formulation of the return mapping algorithms within the mechanical and thermal problems arising from an isentropic split is given in an Appendix.

2. FORMULATION OF THE COUPLED THERMOPLASTIC PROBLEM

We describe below the system of quasi-linear partial differential equations governing the evolution of the coupled thermomechanical initial boundary value problem, including thermal multiphase change and frictional contact constraints.

2.1. Local Governing Equations

Let $2 \leq n_{dim} \leq 3$ be the space dimension and $\mathbb{I} := [0,T] \subset \mathbb{R}_+$ the time interval of interest. Let the open sets $\Omega \subset \mathbb{R}^{n_{dim}}$ with smooth boundary $\partial\Omega$ and closure $\bar{\Omega} := \Omega \cup \partial\Omega$, be the reference placement of a continuum body $\mathcal{B}$.

Denote by $\varphi : \bar{\Omega} \times \mathbb{I} \to \mathbb{R}^{n_{dim}}$ the orientation preserving deformation map of the body $\mathcal{B}$, with material velocity $\boldsymbol{V} := \partial_t \varphi = \dot{\varphi}$, deformation gradient $\boldsymbol{F} := D\varphi$ and absolute

temperature $\Theta : \bar{\Omega} \times \mathbb{I} \to \mathbb{R}$. For each time $t \in \mathbb{I}$, the mapping $t \in \mathbb{I} \mapsto \varphi_t := \varphi(\cdot, t)$ represents a one-parameter family of configurations indexed by time t, which maps the reference placement of body $\mathcal{B}$ onto its current placement $\mathcal{S}_t : \varphi_t(\mathcal{B}) \subset \mathbb{R}^{n_{dim}}$.

The local system of partial differential equations governing the coupled thermomechanical initial boundary value problem is defined by the momentum and energy balance equations, restricted by the inequalities arising from the second law of the thermodynamics. This system must be supplemented by suitable constitutive equations. Additionaly, one must supply suitable prescribed boundary and initial conditions, and consider the equilibrium equations at the contact interfaces.

(A) *Local form of momentum and energy balance equations.* The local form of the momentum and energy balance equations can be written, in a first order system form, as

$$\left.\begin{aligned} \dot{\boldsymbol{\varphi}} &= \boldsymbol{V} \\ \rho_0 \dot{\boldsymbol{V}} &= \mathrm{DIV}[\boldsymbol{\sigma}] + \boldsymbol{B} \\ \Theta \dot{H} &= -\mathrm{DIV}[\boldsymbol{Q}] + R + \mathcal{D}_{int} \end{aligned}\right\} \quad \text{in} \quad \bar{\Omega} \times \mathbb{I} \tag{1}$$

where $\rho_0 : \bar{\Omega} \to \mathbb{R}_+$ is the reference density, $\boldsymbol{B}$ are the (prescribed) body forces per unit reference volume, $\mathrm{DIV}[\cdot]$ the reference divergence operator, $\boldsymbol{\sigma}$ the Cauchy stress tensor, H the entropy per unit reference volume, $\boldsymbol{Q}$ the (nominal) heat flux, R the (prescribed) heat source and $\mathcal{D}_{int}$ the internal dissipation per unit reference volume. Formally, the governing equations for a quasi-static case, may be obtained just by setting $\rho_0 = 0$ in (1).

(B) *Dissipation inequalities.* The specific entropy H and the Cauchy stress tensor $\boldsymbol{\sigma}$ are defined via constitutive relations, typically formulated in terms of the internal energy E, and subjected to the following restriction on the internal dissipation

$$\mathcal{D}_{int} = \boldsymbol{\sigma} : \dot{\boldsymbol{\epsilon}} + \Theta \dot{H} - \dot{E} \geq 0 \qquad \text{in} \quad \bar{\Omega} \times \mathbb{I} \tag{2}$$

where $\boldsymbol{\epsilon} := \mathrm{SYMM}[\boldsymbol{F} - \boldsymbol{I}]$ is the infinitesimal strain tensor. Here $\mathrm{SYMM}[\cdot]$ denotes the symmetric operator and $\boldsymbol{I}$ is the second order identity tensor.

The heat flux $\boldsymbol{Q}$ is defined via constitutive equations, say Fourier's law, subjected to the restriction on the dissipation by conduction

$$\mathcal{D}_{con} = -\frac{1}{\Theta} \mathrm{GRAD}[\Theta] \cdot \boldsymbol{Q} \geq 0 \qquad \text{in} \quad \bar{\Omega} \times \mathbb{I} \tag{3}$$

(C) *Thermoplastic constitutive equations.* Micromechanically based phenomenological models of infinitesimal strain plasticity adopt a local additive decomposition of the strain tensor into elastic and plastic parts. Hardening mechanisms in the material taking place at a microstructural level are characterized by an additional set of phenomenological internal variables collectively denoted here by ξ_α. In the coupled thermomechanical theory, an additive split of the local entropy into elastic and plastic parts is adopted, where the plastic entropy is viewed as an additional internal variable arising as a result of dislocation and lattice defect motion. This additive split of the local entropy was adopted by

ARMERO & SIMO [1993]. The above considerations, motivate the following additive split of the infinitesimal strain tensor $\boldsymbol{\epsilon} := \boldsymbol{\epsilon}^e + \boldsymbol{\epsilon}^p$ and local entropy $H := H^e + H^p$ and the following set of microstructural internal variables $\boldsymbol{G} := \{\boldsymbol{\epsilon}^p, H^p, \xi_\alpha, \}$.

The internal energy function $\hat{E}$ depends on the elastic part of the strain tensor $\boldsymbol{\epsilon}^e$, the hardening internal variables ξ_α and the configurational entropy H^e, taking the functional form $E = \hat{E}(\boldsymbol{\epsilon}^e, H^e, \xi_\alpha,)$. Introducing the functional form of the internal energy into the expression of the internal dissipation, taking the time derivative, applying the chain rule and using the additive split of the infinitesimal strain tensor total entropy, a straightforward argument yields the following constitutive equations and reduced internal dissipation inequality

$$\begin{gathered}\boldsymbol{\sigma} := \partial_{\boldsymbol{\epsilon}^e}\hat{E}(\boldsymbol{\epsilon}^e, H^e, \xi_\alpha), \qquad \Theta := \partial_{H^e}\hat{E}(\boldsymbol{\epsilon}^e, H^e, \xi_\alpha), \qquad \beta^\alpha := -\partial_{\xi_\alpha}\hat{E}(\boldsymbol{\epsilon}^e, H^e, \xi_\alpha), \\ \mathcal{D}_{int} := \mathcal{D}_{mech} + \mathcal{D}_{ther} \geq 0, \quad \text{with} \quad \mathcal{D}_{mech} := \boldsymbol{\sigma} : \dot{\boldsymbol{\epsilon}}^p + \beta^\alpha\, \dot{\xi}_\alpha \geq 0 \quad \text{and} \quad \mathcal{D}_{ther} := \Theta \dot{H}^p.\end{gathered} \tag{4}$$

Using the Legendre transformation $\Psi = E - \Theta H^e$, the free energy function takes the functional form $\Psi = \hat{\Psi}(\boldsymbol{\epsilon}^e, \Theta, \xi_\alpha,)$. Taking the time derivative of the free energy function and applying the chain rule, a straightforward argument yields the following alternative expressions for the constitutive equations

$$\boldsymbol{\sigma} := \partial_{\boldsymbol{\epsilon}^e}\hat{\Psi}(\boldsymbol{\epsilon}^e, \Theta, \xi_\alpha), \qquad H^e := -\partial_\Theta\hat{\Psi}(\boldsymbol{\epsilon}^e, \Theta, \xi_\alpha), \qquad \beta^\alpha := -\partial_{\xi_\alpha}\hat{\Psi}(\boldsymbol{\epsilon}^e, \Theta, \xi_\alpha). \tag{5}$$

Assuming a yield function of the form $\Phi = \hat{\Phi}(\boldsymbol{\sigma}, \beta^\alpha, \Theta)$, the evolution laws of the internal variables, assuming associated flow, take the form

$$\dot{\boldsymbol{\epsilon}}^p := \gamma\, \partial_{\boldsymbol{\sigma}}\hat{\Phi}(\boldsymbol{\sigma}, \beta^\alpha, \Theta), \qquad \dot{\xi}_\alpha := \gamma\, \partial_{\beta^\alpha}\hat{\Phi}(\boldsymbol{\sigma}, \beta^\alpha, \Theta), \qquad \dot{H}^p := \gamma\, \partial_\Theta\hat{\Phi}(\boldsymbol{\sigma}, \beta^\alpha, \Theta), \tag{6}$$

and the following Kuhn-Tucker $\gamma \geq 0, \Phi \leq 0, \gamma\Phi = 0$ and consistency $\gamma\dot{\Phi} = 0$ conditions must be satisfied for a rate-independent plastic model.

Additionally, the heat flux is related to the absolute temperatute through the Fourier's law, that for the isotropic case takes the form $\boldsymbol{Q} = -K\ \mathrm{GRAD}[\Theta]$.

REMARK 1. *Equivalent forms of the energy balance equation.* Using the additive split of the total entropy into elastic and plastic parts and the additive split of the internal dissipation into mechanical and thermal, the reduced energy equation can be expressed as

$$\Theta \dot{H}^e = -\mathrm{DIV}[\boldsymbol{Q}] + R + \mathcal{D}_{mech}. \tag{7}$$

Alternatively, using the constitutive equation of the elastic entropy, taking its time derivative and applying the chain rule, the temperature-form of the reduced energy equation can be written as

$$\begin{gathered}c_0\dot{\Theta} = -\mathrm{DIV}[\boldsymbol{Q}] + R + \mathcal{D}_{mech} - \mathcal{H}^{ep} \qquad \text{with} \\ c_0 := -\Theta\partial^2_{\Theta\Theta}\hat{\Psi}(\boldsymbol{\epsilon}^e, \Theta, \xi_\alpha), \quad \mathcal{H}^{ep} := -\Theta\partial^2_{\Theta\boldsymbol{\epsilon}^e}\hat{\Psi}(\boldsymbol{\epsilon}^e, \Theta, \xi_\alpha) : \dot{\boldsymbol{\epsilon}}^e - \Theta\partial^2_{\Theta\xi_\alpha}\hat{\Psi}(\boldsymbol{\epsilon}^e, \Theta, \xi_\alpha) : \dot{\xi}_\alpha,\end{gathered} \tag{8}$$

where c_0 is the reference heat capacity and $\mathcal{H}^{ep}$ the structural elastoplastic heating. □

REMARK 2. *Thermal phase-change contributions.* The free energy function for a coupled thermomechanical model including phase change can be splitted into thermoelastic Ψ_{te}, thermoplastic Ψ_{tp}, thermal (excluding phase change) Ψ_t and thermal phase change Ψ_{tpc} contributions, taking the functional form, $\Psi = \hat{\Psi}_{te}(\boldsymbol{\epsilon}^e, \Theta) + \hat{\Psi}_{tp}(\Theta, \xi_\alpha) + \hat{\Psi}_t(\Theta) + \hat{\Psi}_{tpc}(\Theta)$.

Collecting into a thermoelastoplastic part $\hat{\Psi}_{tep}(\boldsymbol{\epsilon}^e, \Theta, \xi_\alpha)$ all the terms appearing into the free energy function, excluding the thermal phase change contribution, and setting $H^e := H^e_{tep} + H^e_{tpc}$ with $H^e_{tep} := -\partial_\Theta \hat{\Psi}_{tep}(\boldsymbol{\epsilon}^e, \Theta, \xi_\alpha)$ and $H^e_{tpc} := -\partial_\Theta \hat{\Psi}_{tpc}(\Theta)$, the reduced energy balance equation in entropy form, can be written as

$$\begin{aligned} \Theta \dot{H}^e_{tep} &= -\mathrm{DIV}[\boldsymbol{Q}] + R + \mathcal{D}_{mech} - \mathcal{H}^{pc} \quad \text{with} \\ \mathcal{H}^{pc} :&= \dot{L} = \Theta \dot{H}^e_{tpc} = -\Theta \partial^2_{\Theta\Theta} \hat{\Psi}_{tpc}(\Theta) \cdot \dot{\Theta}, \end{aligned} \tag{9}$$

where $\mathcal{H}^{pc} := \dot{L}$ is the phase-change heating given by the rate of latent heat L per unit reference volume.

Similarly, the reference heat capacity can be splitted into $c_0 = c_{0tep} + c_{0tpc}$ where $c_{0tep} = -\Theta \partial^2_{\Theta\Theta} \hat{\psi}_{tep}(\boldsymbol{\epsilon}^e, \Theta, \xi_\alpha)$ and $c_{0tpc} = -\Theta \partial^2_{\Theta\Theta} \hat{\psi}_{tpc}(\Theta)$, and the temperature form of the energy balance equation takes the form

$$\begin{aligned} c_{0tep} \dot{\Theta} &= -\mathrm{DIV}[\boldsymbol{Q}] + R + \mathcal{D}_{mech} - \mathcal{H}^{ep} - \mathcal{H}^{pc} \quad \text{with} \\ \mathcal{H}^{pc} :&= \dot{L} = c_{0tpc} \dot{\Theta} = -\Theta \partial^2_{\Theta\Theta} \hat{\Psi}_{tpc}(\Theta) \cdot \dot{\Theta}. \ \square \end{aligned} \tag{10}$$

REMARK 3. *Mechanical modeling of the liquid phase.* The mechanical behavior in the liquid, for an isothermal liquid-solid phase change at the solidification (melting) temperature Θ_m, or in the liquid and mushy zone for a non isothermal liquid-solid phase change, given by the liquidus and solidus temperatures Θ_l and Θ_s, respectively, has been modeled by using a modified shear modulus in the liquid phase defined as $G_l = (1 - f_l)G$, where $f_l \in [0, 1]$ is the liquid fraction.

For an isothermal phase change, the liquid fraction takes the form $f_l(\Theta) = H(\Theta - \Theta_m)$, where $H(\cdot)$ is the Heaviside function. In this case, the gradient of the liquid fraction must be interpreted in a distributional sense and takes the form $\nabla f_l(\Theta) = \delta(\Theta - \Theta_m)$, where $\delta(\cdot)$ is the Dirac delta function.

For a non-isothermal phase change, a simple definition of the liquid fraction is a piecewise-linear C^0 function. Alternatively, a C^1 regularized liquid fraction function may be introduced, leading to a more convenient modeling from the point of view of the rate of convergence of the numerical solution. □

2.2. A J2-Thermoplastic constitutive model

Here the following J2-thermoplastic constitutive model described in BOX 1 and BOX 2 has been considered. As it is shown in the model, all the thermomechanical properties may be temperature dependent. A particular interest has been placed in considering the

case in which the specific heat is temperature dependent and the latent heat is non-zero. Note that in this case the functional related to the pure thermal contribution is obtained using an integral expression.

2.3. Thermomechanical contact model

Here only a brief summary of the constitutive thermomechanical contact formulation will be presented. The interested reader is addressed to AGELET DE SARACIBAR [1997A,1997B], and references there in, for further details.

Mechanical contact has been modeled by using a penalty regularization technique. Contact pressure t_N has been characterized by a constitutive equation of the form,

$$t_N = \frac{d}{dg_N} U^+(g_N), \qquad \text{i.e.,} \quad U^+(g_N) = \frac{1}{2}\epsilon_N \langle g_N \rangle^2, \tag{11}$$

where g_N is the normal gap and ϵ_N is a normal penalty parameter.

The frictional constitutive response is governed by the following constrained problem of evolution

$$\left.\begin{aligned} \mathcal{L}_{v_T} \boldsymbol{t}_T^\flat &= \epsilon_T \boldsymbol{v}_T^\flat - \gamma \epsilon_T \partial_{\boldsymbol{t}_T^\flat} \hat{\Phi}(\boldsymbol{t}_T^\flat, t_N, \xi), \\ \dot{\xi} &= \gamma \|\boldsymbol{t}_T^\flat\|, \end{aligned}\right\} \tag{12}$$

where $\boldsymbol{t}_T^\flat$ is the frictional traction, $\boldsymbol{v}_T^\flat$ is the relative slip velocity, ξ is the slip hardening/softening internal variable, here chosen to be the (accumulated) frictional dissipation, ϵ_T is a tangential penalty parameter, $\mathcal{L}_{v_T}(\cdot)$ denotes the Lie derivative along the flow generated by the relative slip velocity and γ and $\hat{\Phi}(\boldsymbol{t}_T^\flat, t_N, \xi)$ are the slip consistency parameter and slip function, respectively, subjected to the following Kuhn-Tucker complementarity and consistency conditions

$$\begin{aligned} &\gamma \geq 0, \quad \hat{\Phi}(\boldsymbol{t}_T^\flat, t_N, \xi) \leq 0, \quad \gamma \hat{\Phi}(\boldsymbol{t}_T^\flat, t_N, \xi) = 0, \\ &\gamma \frac{d}{dt} \hat{\Phi}(\boldsymbol{t}_T^\flat, t_N, \xi) = 0 \quad \text{if} \quad \hat{\Phi}(\boldsymbol{t}_T^\flat, t_N, \xi) = 0. \end{aligned} \tag{13}$$

We refer to LAURSEN [1992], LAURSEN & SIMO [1991,1992,1993A,1993B] and AGELET DE SARACIBAR [1997A,1997B], for further details on the formulation of frictional contact problems.

A thermal contact model at the contact interface is considered, taking into account heat conduction flux through the contact surface, heat generation due to frictional dissipation and heat convection between the interacting bodies when they separate one from each other.

Heat conduction through the contact surface Q_{hcond} has been assumed to be a function of the normal contact pressure t_N, the mean gas temperature Θ_G and the thermal gap g_Θ, of the form

$$Q_{hcond} = \hat{h}_{cond}(t_N, \Theta_G)\ g_\Theta. \tag{14}$$

Heat convection between the two bodies arise when they separate from each other due to a shrinkage process taking place during solidification. Heat convection coefficient has

BOX 1. J2-Thermoplastic constitutive model
Free energy function

■ **Free energy function**

$$\hat{\psi}(\boldsymbol{\epsilon}^e, \xi, \Theta) = \hat{W}(\boldsymbol{\epsilon}^e, \Theta) + \hat{M}(e, \Theta) + \hat{T}(\Theta) + \hat{K}(\xi, \Theta)$$

i. Linear hyperelastic response ($\mu(\Theta) > 0$, $\kappa(\Theta) > 0$),

$$\hat{W}(\boldsymbol{\epsilon}^e, \Theta) = \hat{\bar{W}}(\mathrm{dev}[\boldsymbol{\epsilon}^e], \Theta) + \hat{U}(e, \Theta)$$
$$\hat{\bar{W}}(\mathrm{dev}[\boldsymbol{\epsilon}^e], \Theta) = \mu(\Theta)\ \mathrm{dev}^2[\boldsymbol{\epsilon}^e], \quad \hat{U}(e, \Theta) = \frac{1}{2}\kappa(\Theta) e^2,$$

where $e = \mathrm{tr}[\boldsymbol{\epsilon}^e] = \mathrm{tr}[\boldsymbol{\epsilon}] = \boldsymbol{\epsilon} : \mathbf{1}_3$.

ii. Thermoelastic coupling,

$$\hat{M}(e, \Theta) = -3\kappa(\Theta)\alpha(\Theta)(\Theta - \Theta_0)e.$$

iii. Thermal contribution ($c_s(\Theta) > 0$),

IF ($c_s(\Theta)$=constant AND $L(\Theta) = 0$) THEN

$$\hat{T}(\Theta) = \rho_0 c_s[(\Theta - \Theta_0) - \Theta \log(\Theta/\Theta_0)],$$

ELSE

$$\hat{T}(\Theta) = \int_{\Theta_0}^{\Theta} \hat{T}_{\bar{\Theta}}(\bar{\Theta}) d\bar{\Theta}, \quad \hat{T}_{\bar{\Theta}}(\Theta) = -\int_{\Theta_0}^{\Theta} [\rho_o c_s(\bar{\Theta}) + L'(\bar{\Theta})] \frac{d\bar{\Theta}}{\bar{\Theta}},$$

END IF

iv. Hardening potential,

$$\hat{K}(\xi, \Theta) = \frac{1}{2}h(\Theta)\xi^2 - [y_0(\Theta) - y_\infty(\Theta)]\hat{H}(\xi),$$

where

$$\hat{H}(\xi) := \begin{cases} \xi - (1 - \exp(-\delta\xi))/\delta, & \text{if } \delta \neq 0; \\ 0, & \text{if } \delta = 0. \end{cases}$$

BOX 2. J2-Thermoplastic constitutive model
Thermoelastic and thermoplastic responses

■ **Thermoelastic response**

i. Cauchy stresses,

$$\boldsymbol{\sigma} = p\mathbf{1}_3 + \boldsymbol{s},$$
$$\boldsymbol{s} = 2\mu(\Theta)\mathrm{dev}[\boldsymbol{\epsilon}^e], \quad p = \kappa(\Theta)e - 3\kappa(\Theta)\alpha(\Theta)(\Theta - \Theta_0).$$

ii. Elastic entropy,

IF ($c_s(\Theta)$=constant AND $L(\Theta) = 0$) THEN

$$H^e = \rho_0 c_s \log(\Theta/\Theta_0) + 3\kappa(\Theta)\alpha(\Theta)e - \hat{K}_\Theta(\xi)$$
$$- \hat{W}_\Theta(\boldsymbol{\epsilon}^e, \Theta) + 3[\kappa(\Theta)\alpha'(\Theta) + \kappa'(\Theta)\alpha(\Theta)](\Theta - \Theta_0)e,$$

ELSE

$$H^e = \int_{\Theta_0}^{\Theta} [\rho_0 c_s(\bar{\Theta}) + L'(\bar{\Theta})]\frac{d\bar{\Theta}}{\bar{\Theta}} + 3\kappa(\Theta)\alpha(\Theta)e - \hat{K}_\Theta(\xi)$$
$$- \hat{W}_\Theta(\boldsymbol{\epsilon}^e, \Theta) + 3[\kappa(\Theta)\alpha'(\Theta) + \kappa'(\Theta)\alpha(\Theta)](\Theta - \Theta_0)e,$$

END IF

■ **Thermoplastic response**

i. Von Mises yield criterion with flow stress $\sigma_Y(\Theta) := y_0(\Theta)$,

$$\hat{\phi}(\boldsymbol{\sigma}, q, \Theta) = \|\mathrm{dev}[\boldsymbol{\sigma}]\| - \sqrt{\frac{2}{3}}[\sigma_Y(\Theta) - q] \leq 0.$$

ii. Hardening variable q conjugate to ξ,

$$q := -\partial_\xi \hat{\psi} = -[h(\Theta)\xi - (y_0(\Theta) - y_\infty(\Theta))(1 - \exp(-\delta\xi))].$$

iii. Linear thermal softening,

$$\left.\begin{aligned} y_0(\Theta) &= y_0(\Theta_0)[1 - w_0(\Theta - \Theta_0)], \\ y_\infty(\Theta) &= y_\infty(\Theta_0)[1 - w_\infty(\Theta - \Theta_0)], \\ h(\Theta) &= h(\Theta_0)[1 - w_h(\Theta - \Theta_0)]. \end{aligned}\right\}$$

been assumed to be a function of the mechanical gap. Then the heat convection has been assumed to be modeled as

$$Q_{hconv} = \hat{h}_{conv}(g_N)\, g_\Theta. \tag{15}$$

We refer to WRIGGERS & MIEHE [1992,1994] and AGELET DE SARACIBAR [1997B] for further details on the formulation of thermal contact models and thermomechanical contact formulations.

2.4. Variational formulation

Using standard procedures, the weak form of the momentum balance (we will assume the quasi-static case for simplicity) and reduced energy equations take the following expressions:

$$\begin{aligned} \langle \boldsymbol{\sigma}, \mathrm{GRAD}[\eta_0] \rangle &= \langle \boldsymbol{B}, \eta_0 \rangle + \langle \bar{\boldsymbol{t}}, \eta_0 \rangle_{\Gamma_\sigma} + \langle \boldsymbol{t}, \eta_0 \rangle_{\Gamma_{mc}} \\ \langle \Theta \dot{H}^e, \zeta_0 \rangle - \langle \boldsymbol{Q}, \mathrm{GRAD}[\zeta_0] \rangle &= \langle R + \mathcal{D}_{mech}, \zeta_0 \rangle - \langle \bar{Q}, \zeta_0 \rangle_{\Gamma_Q} - \langle Q, \zeta_0 \rangle_{\Gamma_{tc}} \end{aligned} \tag{16}$$

which must hold for any admissible displacement and temperature functions η_0 and ζ_0, respectively. We refer to AGELET DE SARACIBAR [1997B] for notation and further details on the derivation of these weak forms and, particularly, on the expressions related to the thermomechanical frictional contact constributions.

3. TIME INTEGRATION OF THE COUPLED THERMOPLASTIC PROBLEM

The numerical solution of the coupled thermomechanical IBVP involves the transformation of an infinite dimensional dynamical system, governed by a system of quasi-linear partial differential equations into a sequence of discrete nonlinear algebraic problems by means of a Galerkin finite element projection and a time marching scheme for the advancement of the primary nodal variables, i.e. displacements and temperatures, together with a return mapping algorithm for the advancement of the internal variables.

Here, attention will be placed to the time integration schemes of the governing equations of the coupled thermoplastic problem. In particular, we are interested in a class of unconditionally stable staggered solution schemes, based on a *product formula algorithm* arising from an operator split of the governing evolution equations. These methods fall within the classical *fractional step methods.*

3.1. Local evolution problem

Consider the following (homogeneous) first order constrained dissipative local problem of evolution

$$\left.\begin{aligned} \frac{d}{dt}\boldsymbol{Z} &= \boldsymbol{A}[\boldsymbol{Z}, \boldsymbol{\Gamma}] \quad \text{in} \quad \bar{\Omega} \times [0,T], \\ \boldsymbol{Z}|_{t=0} &= \boldsymbol{Z}_0 \qquad\quad \text{in} \quad \bar{\Omega}, \end{aligned}\right\} \tag{17}$$

along with

$$\left.\begin{array}{ll} \dfrac{d}{dt}\boldsymbol{\Gamma} = \gamma\, \boldsymbol{G}[\boldsymbol{Z},\boldsymbol{\Gamma}] & \text{in } \bar{\Omega}\times[0,T], \\ \boldsymbol{\Gamma}|_{t=0} = 0 & \text{in } \bar{\Omega}, \end{array}\right\} \tag{18}$$

where $\boldsymbol{Z}$, lying in a suitable Sobolev space $\mathcal{Z}$, is a set of primary independent variables, $\boldsymbol{\Gamma}$ is a set of internal variables, $\boldsymbol{A}[\boldsymbol{Z},\boldsymbol{\Gamma}]$ and $\boldsymbol{G}[\boldsymbol{Z},\boldsymbol{\Gamma}]$ are nonlinear operators and $\gamma \geq 0$ is a multiplier subjected to the classical Kuhn-Tucker conditions for a rate-independent plasticity model. In the formulation of the fractional step method described below, it is essential to regard the set of internal variables $\boldsymbol{\Gamma}$ as *implicitly defined* in terms of the variables $\boldsymbol{Z}$ via the evolution equations (18). Therefore $\boldsymbol{Z}$ are the only independent variables and their choice becomes a crucial aspect in the formulation of the fractional step method. We refer to SIMO [1994] for further details.

Consider the set of *conservation/entropy/latent heat* variables $\boldsymbol{Z}$ and the set of internal variables $\boldsymbol{\Gamma}$ defined, respectively, as

$$\boxed{\boldsymbol{Z} := \{\boldsymbol{\varphi}, \boldsymbol{p}, H^e, H^p, L\} \qquad \text{and} \qquad \boldsymbol{\Gamma} := \{\boldsymbol{\epsilon}^p, \xi_\alpha\}} \tag{19}$$

where $\boldsymbol{\varphi}$ is the deformation map, $\boldsymbol{p} := \rho_0 \boldsymbol{V}$ denotes the material linear momentum, H^e and H^p are the elastic entropy (including phase change contributions) and plastic entropy per unit reference volume, respectively, L is the latent heat per unit reference volume, $\boldsymbol{\epsilon}^p$ the plastic strain and ξ_α the strain-like hardening variables. The choice of $\boldsymbol{Z}$ becomes motivated by the design constraints introduced in the isentropic operator split described below.

All the remaining variables in the problem can be defined in terms of $\boldsymbol{Z}$ and $\boldsymbol{\Gamma}$ by kinematic and constitutive equations. In particular,

i. The elastic strain $\boldsymbol{\epsilon}^e := \boldsymbol{\epsilon} - \boldsymbol{\epsilon}^p$.

ii. The Cauchy stress tensor $\boldsymbol{\sigma} := \partial_{\boldsymbol{\epsilon}^e} \hat{E}(\boldsymbol{\epsilon}^e, H^e, \xi_\alpha)$ and stress-like hardening variables $\beta^\alpha := -\partial_{\xi_\alpha} \hat{E}(\boldsymbol{\epsilon}^e, H^e, \xi_\alpha)$.

iii. The temperature $\Theta := \partial_{H^e} \hat{E}(\boldsymbol{\epsilon}^e, H^e, \xi_\alpha)$ and nominal heat flux $\boldsymbol{Q} = -K\ \mathrm{GRAD}[\Theta]$.

With these definitions in hand, and assuming zero body forces and zero heat sources, the governing evolution equations of the thermoplastic problem can be written in the form given by (17)-(18) where the nonlinear operators $\boldsymbol{A}[\boldsymbol{Z},\boldsymbol{\Gamma}]$ and $\boldsymbol{G}[\boldsymbol{Z},\boldsymbol{\Gamma}]$ take the form

$$\boldsymbol{A}[\boldsymbol{Z},\boldsymbol{\Gamma}] := \left\{\begin{array}{c} \frac{1}{\rho_0}\boldsymbol{p} \\ \mathrm{DIV}[\boldsymbol{\sigma}] \\ -\frac{1}{\Theta}\ \mathrm{DIV}[\boldsymbol{Q}] + \frac{1}{\Theta}\ \mathcal{D}_{mech} \\ \frac{1}{\Theta}\ \mathcal{D}_{ther} \\ \mathcal{H}^{pc} \end{array}\right\}, \qquad \boldsymbol{G}[\boldsymbol{Z},\boldsymbol{\Gamma}] := \left\{\begin{array}{c} \partial_{\boldsymbol{\sigma}}\hat{\Phi}(\boldsymbol{\sigma}, \beta^\alpha, \Theta) \\ \partial_{\beta^\alpha}\hat{\Phi}(\boldsymbol{\sigma}, \beta^\alpha, \Theta) \end{array}\right\}, \tag{20}$$

where the phase-change heating $\mathcal{H}^{pc}$ is given by

$$\mathcal{H}^{pc} := -\Theta \partial^2_{\Theta\Theta} \hat{\Psi}_{tpc}(\Theta) \cdot \dot{\Theta}, \tag{21}$$

and the mechanical dissipation $\mathcal{D}_{mech}$ and thermal dissipation $\mathcal{D}_{ther}$ are given by

$$\mathcal{D}_{mech} := \gamma \boldsymbol{\Sigma} : \boldsymbol{G}[\boldsymbol{Z},\boldsymbol{\Gamma}] \geq 0, \qquad \mathcal{D}_{ther} := \gamma \Theta \partial_\Theta \hat{\Phi}(\boldsymbol{\sigma}, \beta^\alpha, \Theta), \tag{22}$$

where, using a compact notation, we denoted as $\boldsymbol{\Sigma}^T := [\boldsymbol{\sigma}^T, \beta^\alpha]$ the generalized stresses.

3.2. A-priori stability estimate

For nonlinear *dissipative* problems of evolution *nonlinear stability* can be phrased in terms of an *a-priori estimate* on the dynamics of the form

$$\boxed{\frac{d}{dt}\mathcal{L}(\boldsymbol{Z},\boldsymbol{\Gamma}) \leq 0 \quad \text{for} \quad t \in [0,T]} \tag{23}$$

where $\mathcal{L}(\cdot)$ is a *non-negative Lyapunov*-like function.

For nonlinear thermoplasticity, see ARMERO & SIMO [1993], consider an extended canonical free energy functional $\mathcal{L}(\cdot)$ defined as

$$\mathcal{L}(\boldsymbol{Z},\boldsymbol{\Gamma}) = \int_\Omega [\frac{|\boldsymbol{p}|^2}{2\rho_0} + \hat{E}(\boldsymbol{\epsilon}^e, H^e, \xi_\alpha) - \Theta_0 H^e] d\Omega + V_{ext}(\boldsymbol{\varphi}), \tag{24}$$

and assume that the following conditions hold,

i. Zero heat sources, i.e., $R = 0$,
ii. Conservative mechanical loading with potential $V_{ext}(\boldsymbol{\varphi})$, i.e. $\boldsymbol{B} = -\partial_{\boldsymbol{\varphi}} V_{ext}(\boldsymbol{\varphi})$,
iii. Dirichlet boundary conditions for the temperature field with prescribed constant temperature $\Theta_0 > 0$, i.e., $\Theta = \Theta_0$ on $\partial\Omega \times \mathbb{I}$ and $\Gamma_Q = \emptyset$.

Then, $\mathcal{L}(\cdot)$ is a *non-increasing Lyapunov*-like function along the flow generated by the thermoplastic problem and a straightforward computation shows that the following *a-priori stability estimate* holds:

$$\boxed{\frac{d}{dt}\mathcal{L}(\boldsymbol{Z},\boldsymbol{\Gamma}) = -\int_\Omega \frac{\Theta_0}{\Theta}[\mathcal{D}_{mech} + \mathcal{D}_{con}] d\Omega \leq 0 \ \text{ in } [0,T].} \tag{25}$$

This condition is regarded, see ARMERO & SIMO [1993], as a *fundamental a-priori estimate* for the thermoplastic problem of evolution which *must be preserved* by the time-stepping algorithm.

3.3. Operator splits

Consider the dissipative problem of evolution given by (17)-(18) with the associated non-increasing Lyapunov-like function $\mathcal{L}(\cdot)$ given by (24). Consider an additive operator split of the vector field $\boldsymbol{A} = \boldsymbol{A}^{(1)} + \boldsymbol{A}^{(2)}$ leading to the following two sub-problems

$$\begin{array}{ll} \underline{\text{Problem 1}} & \underline{\text{Problem 2}} \\ \left.\begin{array}{l} \dot{\boldsymbol{Z}} = \boldsymbol{A}^{(1)}[\boldsymbol{Z},\boldsymbol{\Gamma}], \\ \dot{\boldsymbol{\Gamma}} = \gamma\, \boldsymbol{G}[\boldsymbol{Z},\boldsymbol{\Gamma}], \end{array}\right\} & \left.\begin{array}{l} \dot{\boldsymbol{Z}} = \boldsymbol{A}^{(2)}[\boldsymbol{Z},\boldsymbol{\Gamma}], \\ \dot{\boldsymbol{\Gamma}} = \gamma\, \boldsymbol{G}[\boldsymbol{Z},\boldsymbol{\Gamma}]. \end{array}\right\} \end{array} \tag{26}$$

The *critical restriction on the design of the operator split* is that each one of the sub-problems *must preserve the underlying dissipative structure of the original problem*, i.e.,

$$\boxed{\frac{d}{dt}\mathcal{L}(\boldsymbol{Z}^{(\alpha)},\boldsymbol{\Gamma}^{(\alpha)}) \leq 0, \quad \alpha = 1,2.} \tag{27}$$

where $t \mapsto (\boldsymbol{Z}^{(\alpha)}, \boldsymbol{\Gamma}^{(\alpha)})$ denotes the flow generated by the vector field $\boldsymbol{A}^{(\alpha)}$, $\alpha = 1, 2$.

Two different operator splits will be considered here. First, following ARMERO & SIMO [1992A,1992B,1993], an isentropic operator split, which satisfies the critical design restriction mentioned above, is considered. This split is compared next with an isothermal operator split, which does not satisfy the design restriction.

(A) *The isentropic operator split.* Consider the following additive *isentropic*-based operator split of the vector field $\boldsymbol{A}[\boldsymbol{Z}, \boldsymbol{\Gamma}]$:

$$\boldsymbol{A}[\boldsymbol{Z}, \boldsymbol{\Gamma}] := \boldsymbol{A}^{(1)}_{ise}[\boldsymbol{Z}, \boldsymbol{\Gamma}] + \boldsymbol{A}^{(2)}_{ise}[\boldsymbol{Z}, \boldsymbol{\Gamma}], \tag{28}$$

where we define the vector fields $\boldsymbol{A}^{(1)}_{ise}$ and $\boldsymbol{A}^{(2)}_{ise}$ as

$$\boldsymbol{A}^{(1)}_{ise}[\boldsymbol{Z}, \boldsymbol{\Gamma}] := \left\{ \begin{array}{c} \frac{1}{\rho_0}\boldsymbol{p} \\ \mathrm{DIV}[\boldsymbol{\sigma}] \\ 0 \\ 0 \\ 0 \end{array} \right\}, \qquad \boldsymbol{A}^{(2)}_{ise}[\boldsymbol{Z}, \boldsymbol{\Gamma}] := \left\{ \begin{array}{c} 0 \\ 0 \\ -\frac{1}{\Theta}\mathrm{DIV}[\boldsymbol{Q}] + \frac{1}{\Theta}\mathcal{D}_{mech} \\ \frac{1}{\Theta}\mathcal{D}_{ther} \\ \mathcal{H}^{pc} \end{array} \right\}, \tag{29}$$

and consider the following two problems of evolution:

$$\begin{array}{ll} \underline{\textit{Problem 1}} & \underline{\textit{Problem 2}} \\ \left. \begin{array}{l} \dot{\boldsymbol{Z}} = \boldsymbol{A}^{(1)}_{ise}[\boldsymbol{Z}, \boldsymbol{\Gamma}], \\ \dot{\boldsymbol{\Gamma}} = \gamma\, \boldsymbol{G}[\boldsymbol{Z}, \boldsymbol{\Gamma}], \end{array} \right\} & \left. \begin{array}{l} \dot{\boldsymbol{Z}} = \boldsymbol{A}^{(2)}_{ise}[\boldsymbol{Z}, \boldsymbol{\Gamma}], \\ \dot{\boldsymbol{\Gamma}} = \gamma\, \boldsymbol{G}[\boldsymbol{Z}, \boldsymbol{\Gamma}]. \end{array} \right\} \end{array} \tag{30}$$

Within this operator split, *Problem* 1 defines a mechanical phase at fixed entropy and *Problem* 2 defines a thermal phase at fixed configuration. Note that a strong condition has been placed in the *Problem* 1, by the additional requirement that not only the entropy must remain fixed, but also the elastic and plastic entropy, as well as the latent heat, must remain fixed. Note also that the evolution of the plastic internal variables $\boldsymbol{\Gamma}$ is imposed in both problems.

Denoting by $t \mapsto (\boldsymbol{Z}^{(\alpha)}, \boldsymbol{\Gamma}^{(\alpha)})$ the flow generated by the vector field $\boldsymbol{A}^{(\alpha)}_{ise}$, $\alpha = 1, 2$, a straightforward computation shows that the following estimates hold:

$$\boxed{\begin{array}{l} \dfrac{d}{dt}\mathcal{L}(\boldsymbol{Z}^{(1)}, \boldsymbol{\Gamma}^{(1)}) = -\displaystyle\int_{\Omega} \mathcal{D}^{(1)}_{mech} d\Omega \leq 0, \\ \dfrac{d}{dt}\mathcal{L}(\boldsymbol{Z}^{(2)}, \boldsymbol{\Gamma}^{(2)}) = -\displaystyle\int_{\Omega} \frac{\Theta_0}{\Theta^{(2)}}[\mathcal{D}^{(2)}_{mech} + \mathcal{D}^{(2)}_{con}] d\Omega \leq 0, \end{array}} \tag{31}$$

where $\mathcal{D}^{(\alpha)}_{mech}$, $\mathcal{D}^{(\alpha)}_{con}$ and $\Theta^{(\alpha)}$ are the mechanical dissipation, thermal heat conduction dissipation and absolute temperature, respectively, in *Problem* α, $\alpha = 1, 2$.

Thus, the isentropic split preserves the underlying dissipative structure of the original problem.

(B) *The isothermal operator split.* Consider the following additive *isothermal*-based operator split of the vector field $\boldsymbol{A}[\boldsymbol{Z},\boldsymbol{\Gamma}]$:

$$\boldsymbol{A}[\boldsymbol{Z},\boldsymbol{\Gamma}] := \boldsymbol{A}^{(1)}_{iso}[\boldsymbol{Z},\boldsymbol{\Gamma}] + \boldsymbol{A}^{(2)}_{iso}[\boldsymbol{Z},\boldsymbol{\Gamma}], \tag{32}$$

where we define the vector fields $\boldsymbol{A}^{(1)}_{iso}$ and $\boldsymbol{A}^{(2)}_{iso}$ as

$$\boldsymbol{A}^{(1)}_{iso}[\boldsymbol{Z},\boldsymbol{\Gamma}] := \left\{ \begin{array}{c} \frac{1}{\rho_0}\boldsymbol{p} \\ \mathrm{DIV}[\boldsymbol{\sigma}] \\ \frac{1}{\Theta}\mathcal{H}^{ep} \\ 0 \\ 0 \end{array} \right\}, \qquad \boldsymbol{A}^{(2)}_{iso}[\boldsymbol{Z},\boldsymbol{\Gamma}] := \left\{ \begin{array}{c} 0 \\ 0 \\ -\frac{1}{\Theta}\mathrm{DIV}[\boldsymbol{Q}] + \frac{1}{\Theta}(\mathcal{D}_{mech} - \mathcal{H}^{ep}) \\ \frac{1}{\Theta}\mathcal{D}_{ther} \\ \mathcal{H}^{pc} \end{array} \right\}, \tag{33}$$

and consider the following two problems of evolution:

$$\begin{array}{ll} \underline{\textit{Problem 1}} & \underline{\textit{Problem 2}} \\ \left. \begin{array}{l} \dot{\boldsymbol{Z}} = \boldsymbol{A}^{(1)}_{iso}[\boldsymbol{Z},\boldsymbol{\Gamma}], \\ \dot{\boldsymbol{\Gamma}} = \gamma\, \boldsymbol{G}[\boldsymbol{Z},\boldsymbol{\Gamma}], \end{array} \right\} & \left. \begin{array}{l} \dot{\boldsymbol{Z}} = \boldsymbol{A}^{(2)}_{iso}[\boldsymbol{Z},\boldsymbol{\Gamma}], \\ \dot{\boldsymbol{\Gamma}} = \gamma\, \boldsymbol{G}[\boldsymbol{Z},\boldsymbol{\Gamma}]. \end{array} \right\} \end{array} \tag{34}$$

Within this operator split, *Problem* 1 defines a mechanical phase at fixed temperature and *Problem* 2 defines a thermal phase at fixed configuration. Note also, that the evolution of the plastic internal variables $\boldsymbol{\Gamma}$ is imposed in both problems.

Denoting by $t \mapsto (\boldsymbol{Z}^{(\alpha)}, \boldsymbol{\Gamma}^{(\alpha)})$ the flow generated by the vector field $\boldsymbol{A}^{(\alpha)}_{iso}$, $\alpha = 1, 2$, a straightforward computation shows that the following estimates hold:

$$\boxed{\begin{array}{l} \dfrac{d}{dt}\mathcal{L}(\boldsymbol{Z}^{(1)}, \boldsymbol{\Gamma}^{(1)}) = -\displaystyle\int_{\Omega} \mathcal{D}^{(1)}_{mech} d\Omega + \int_{\Omega} (1 - \frac{\Theta_0}{\Theta^{(1)}}) \mathcal{H}^{ep(1)} d\Omega \lesssim 0, \\ \dfrac{d}{dt}\mathcal{L}(\boldsymbol{Z}^{(2)}, \boldsymbol{\Gamma}^{(2)}) = -\displaystyle\int_{\Omega} \frac{\Theta_0}{\Theta^{(2)}} [\mathcal{D}^{(2)}_{mech} + \mathcal{D}^{(2)}_{con}] d\Omega - \int_{\Omega} (1 - \frac{\Theta_0}{\Theta^{(2)}}) \mathcal{H}^{ep(2)} d\Omega \lesssim 0, \end{array}} \tag{35}$$

where $\mathcal{D}^{(\alpha)}_{mech}$, $\mathcal{D}^{(\alpha)}_{con}$, $\mathcal{H}^{ep(\alpha)}$ and $\Theta^{(\alpha)}$ are the mechanical dissipation, thermal heat conduction dissipation, structural elastoplastic heating and absolute temperature, respectively, in *Problem* α, $\alpha = 1, 2$.

The contribution of the *structural elastoplastic heating* to the evolution equations of each one of the problems arising from the isothermal operator split, *breaks the underlying dissipative structure of the original problem.*

3.4. Product formula algorithms

The additive operator split of the governing evolution equations leads to a product formula algorithm and to a staggered solution scheme of the coupled problem, in which each one of the subproblems is solved sequentially. Remember that the set of internal variables $\boldsymbol{\Gamma}$ is viewed as implicitly defined in terms of the set of variables $\boldsymbol{Z}$, which are

considered to be the only independent variables. Therefore, our interest here is placed on the time discrete version of the evolution equation (17), and the update in time of the variables $\boldsymbol{Z}$ using a time-stepping algorithm.

Consider algorithms $\mathbb{K}^{(\alpha)}_{\Delta t}[\cdot]$ being *consistent* with the flows $t \mapsto (\boldsymbol{Z}^{(\alpha)}, \boldsymbol{\Gamma}^{(\alpha)})$, $\alpha = 1, 2$, and *dissipative stables*, i.e. which inherit the a-priori stability estimate on the dynamics given by (27). Then the algorithm defined by the *product formula*:

$$\mathbb{K}_{\Delta t}[\cdot] = \left(\mathbb{K}^{(2)}_{\Delta t} \circ \mathbb{K}^{(1)}_{\Delta t}\right)[\cdot] \tag{36}$$

is also *consistent* and *dissipative stable*. For *dissipative dynamical systems* if each of the algorithms is unconditionally dissipative stable, then the *product formula algorithm* is also unconditionally dissipative stable. This product formula algorithm is only *first order accurate*. A second order accurate product formula algorithm can be defined through a *double pass technique* given by, see STRANG [1969],

$$\mathbb{K}_{\Delta t}[\cdot] = \left(\mathbb{K}^{(1)}_{\Delta t/2} \circ \mathbb{K}^{(2)}_{\Delta t} \circ \mathbb{K}^{(1)}_{\Delta t/2}\right)[\cdot]. \tag{37}$$

Note that, according to (31) and (35), algorithms based on the isothermal operator split will result in staggered schemes at best only conditionally stables and only an isentropic operator split leads to unconditionally (dissipative) stable product formula algorithms.

3.5. Time discrete variational formulation

The use of an *operator split*, applied to the coupled system of nonlinear ordinary differential equations, and a *product formula algorithm*, leads to a *staggered algorithm* in which each one of the subproblems defined by the partition is solved sequentially, within the framework of classical *fractional step methods*. We note that contrary to common practice, the evolution equations for the microstructural internal variables are enforced in both phases of the operator split. A Backward-Euler (BE) time stepping algorithm has been used and two different operator splits have been considered:

(A) *Isentropic split*. In the *isentropic split*, first introduced by ARMERO & SIMO [1992,1993], the coupled problem is partitioned into a mechanical phase at constant entropy, followed by a thermal phase at fixed configuration, leading to an unconditionally stable staggered scheme. The additional design constraints of constant elastic and plastic entropy and latent heat, in the isentropic mechanical phase have been introduced. An efficient implementation of the split can be done using the temperature as primary variable. See ARMERO & SIMO [1992A,1992B,1993] and SIMO [1994] for further details.

i. *Mechanical phase*. The mechanical problem is solved at constant entropy. For the sake of simplicity, only the quasi-static case will be considered. According to the definition of $\boldsymbol{Z}$ given by (19) and the operator split given by (28)-(30), the additional design constraints of constant elastic and plastic entropy and latent heat, have been introduced. The evolution of the temperature can be computed locally. The time discrete weak form

of the momentum balance and the local updates of elastic and plastic entropy, latent heat and internal variables, take the form:

$$\left.\begin{aligned} \langle \tilde{\boldsymbol{\sigma}}_{n+1}, \mathrm{GRAD}[\boldsymbol{\eta}_0] \rangle &= \langle \boldsymbol{B}, \boldsymbol{\eta}_0 \rangle + \langle \bar{\boldsymbol{t}}_{n+1}, \boldsymbol{\eta}_0 \rangle_{\Gamma_\sigma} + \langle \boldsymbol{t}_{n+1}, \boldsymbol{\eta}_0 \rangle_{\Gamma_{mc}} \\ \tilde{H}^e_{n+1} &= H^e_n, \\ \tilde{H}^p_{n+1} &= H^p_n, \\ \tilde{L}_{n+1} &= L_n, \\ \tilde{\boldsymbol{\Gamma}}_{n+1} &= \boldsymbol{\Gamma}_n + \tilde{\gamma}_{n+1}\, \tilde{\boldsymbol{G}}_{n+1}, \end{aligned}\right\} \tag{38}$$

and the temperature is locally updated according to $\tilde{\Theta}_{n+1} = \partial_{H^e} \hat{E}(\tilde{\boldsymbol{\epsilon}}^e_{n+1}, H^e_n, \tilde{\xi}_{\alpha n+1})$.

ii. *Thermal phase.* Using a BE scheme the time discrete weak form of the energy balance equation and updated elastic and plastic entropy, latent heat and internal variables in the thermal phase take the form:

$$\left.\begin{aligned} \frac{1}{\Delta t} \langle \Theta_{n+1}(H^e_{n+1} - H^e_n), \zeta_0 \rangle - \langle \boldsymbol{Q}_{n+1}, \mathrm{GRAD}[\zeta_0] \rangle &= \\ \langle R + \mathcal{D}_{mech\, n+1}, \zeta_0 \rangle - \langle \bar{Q}_{n+1}, \zeta_0 \rangle_{\Gamma_Q} - \langle Q_{n+1}, \zeta_0 \rangle_{\Gamma_{tc}} & \\ H^e_{n+1} = -\partial_\Theta \hat{\Psi}(\boldsymbol{\epsilon}^e_{n+1}, \Theta_{n+1}, \xi_{\alpha n+1}), & \\ H^p_{n+1} = H^p_n + \frac{\Delta t}{\Theta_{n+1}} \mathcal{D}_{ther\, n+1}, & \\ L_{n+1} = L(\Theta_{n+1}), & \\ \boldsymbol{\Gamma}_{n+1} = \boldsymbol{\Gamma}_n + \gamma_{n+1}\, \boldsymbol{G}_{n+1}. & \end{aligned}\right\} \tag{39}$$

(B) *Isothermal split.* In the isothermal split the coupled system of equations is partitioned into a mechanical phase at constant temperature, followed by a thermal phase at fixed configuration. Note that, within the context of the product formula algorithm, using the entropy form of the energy equation, the elastic entropy computed at the end of the mechanical partition is used as initial condition for the solution of the thermal partition.

i. *Mechanical phase.* Noting that under isothermal conditions the plastic entropy and latent heat remain constant, the time discrete weak form of the momentum balance equation, updated elastic and plastic entropy, latent heat and internal variables take the form:

$$\left.\begin{aligned} \langle \tilde{\boldsymbol{\sigma}}_{n+1}, \mathrm{GRAD}[\boldsymbol{\eta}_0] \rangle &= \langle \boldsymbol{B}, \boldsymbol{\eta}_0 \rangle + \langle \bar{\boldsymbol{t}}_{n+1}, \boldsymbol{\eta}_0 \rangle_{\Gamma_\sigma} + \langle \boldsymbol{t}_{n+1}, \boldsymbol{\eta}_0 \rangle_{\Gamma_{mc}} \\ \tilde{H}^e_{n+1} &= -\partial_\Theta \hat{\Psi}(\tilde{\boldsymbol{\epsilon}}^e_{n+1}, \Theta_n, \tilde{\xi}_{\alpha n+1}), \\ \tilde{H}^p_{n+1} &= H^p_n, \\ \tilde{L}_{n+1} &= L_n, \\ \tilde{\boldsymbol{\Gamma}}_{n+1} &= \boldsymbol{\Gamma}_n + \tilde{\gamma}_{n+1}\, \tilde{\boldsymbol{G}}_{n+1}, \end{aligned}\right\} \tag{40}$$

and the temperature remains constant $\tilde{\Theta}_{n+1} = \Theta_n$.

ii. *Thermal phase.* Using a BE scheme the time discrete weak form of the energy balance equation and updated elastic and plastic entropy, latent heat and internal variables take the form:

$$\left.\begin{aligned}
&\frac{1}{\Delta t}\langle \Theta_{n+1}(H^e_{n+1} - \tilde{H}^e_{n+1}), \zeta_0\rangle - \langle \boldsymbol{Q}_{n+1}, \mathrm{GRAD}[\zeta_0]\rangle = \\
&\qquad\qquad \langle R + \mathcal{D}_{mechn+1} - \mathcal{H}^{ep}_{n+1}, \zeta_0\rangle - \langle \bar{Q}_{n+1}, \zeta_0\rangle_{\Gamma_Q} - \langle Q_{n+1}, \zeta_0\rangle_{\Gamma_{tc}} \\
&H^e_{n+1} = -\partial_\Theta \hat{\Psi}(\epsilon^e_{n+1}, \Theta_{n+1}, \xi_{\alpha n+1}), \\
&H^p_{n+1} = H^p_n + \frac{\Delta t}{\Theta_{n+1}} \mathcal{D}_{thern+1}, \\
&L_{n+1} = L(\Theta_{n+1}), \\
&\boldsymbol{\Gamma}_{n+1} = \boldsymbol{\Gamma}_n + \gamma_{n+1}\, \boldsymbol{G}_{n+1}.
\end{aligned}\right\} \tag{41}$$

4. NUMERICAL SIMULATIONS

The formulation presented in the previous Sections is illustrated here in a number of representative numerical simulations. First a numerical assessment of the accuracy and stability behavior of the isothermal and isentropic operator splits is presented in the context of quasi-static and fully dynamic cooling analysis of a thermoelastic and thermoplastic pressurized thick walled cylinder. Next, the goals are to provide a practical accuracy assessment of the thermomechanical model and to demonstrate the robustness of the overall coupled thermomechanical formulation in a number of solidification examples, including industrial processes. The computations are performed with the finite element code COMET developed by the authors. The Newton-Raphson method, combined with a line search optimization procedure, is used to solve the nonlinear system of equations arising from the spatial and temporal discretization of the weak form of the momentum and reduced dissipation balance equations. Convergence of the incremental iterative solution procedure was monitored by requiring a tolerance of 0.1% in the residual based error norm.

4.1. Numerical assessment of the operator split algorithms

(A) *Cooling of a thermoelastic/thermoplastic thick walled cylinder.* In this problem a quasi-static and fully dynamic cooling analysis of a thermoelastic and thermoplastic pressurized thick walled cylinder is presented. The goals here are to provide a numerical assessment of the accuracy and stability behavior showed by the isothermal and isentropic operator splits, in weakly (Case 1) and strongly (Case 2) coupled problems. To get a strongly coupled problem, the thermal expansion coefficient α has been, unrealistically, multiplied by a factor of 6 in the quasi-static cases and by a factor of 3 in the fully dynamic cases.

FIGURE 4.1 depicts the initial geometry of the problem, as well as the prescribed boundary conditions. Plane strain conditions are assumed in the axial direction, so that a unit band of axisymmteric finite elements need only be condidered. The inner and outer radii adopted are $R_i = 100$ mm and $R_o = 200$ mm, respectively. The material

properties are assumed to be (linearly) temperature dependent. The initial temperature of the cylinder is 593 °K, while the reference (ambient) temperature is 293 °K. Different (constant) convection coefficients are considered for the inner, $h = 1.16$ N/mm s °K, and outer, $h = 0.01$ N/mm s K, surfaces. The simulations are performed by applying a pressure of 200 N/mm^2 at the inner face of the cylinder. Standard bi-linear isoparametric axisymmetric finite elements are employed.

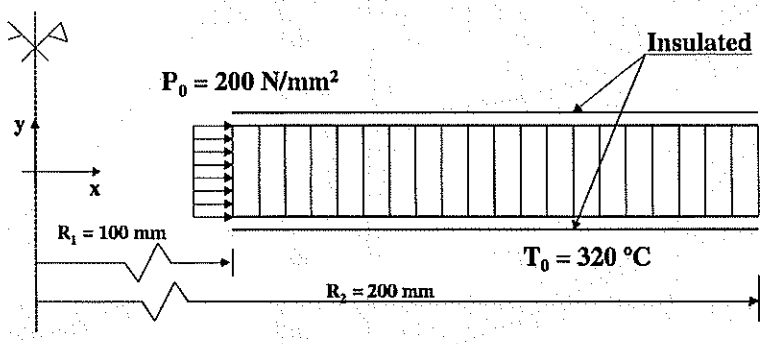

FIGURE 4.1. Cooling of a pressurized thick-walled cylinder. Initial geometry and boundary conditions.

The results obtained for the quasi-static analyses are collected in FIGURES 4.2 and 4.3 for a thermoelastic and a thermoplastic constitutive response, respectively. FIGURES 4.4 and 4.5 collect the results obtained for the fully dynamic analysis, assuming a thermoelastic and a thermoplastic constitutive response, respectively. In each of these Figures, it is shown for the Cases 1 and 2, the radial displacement and temperature evolutions at the inner and outer surfaces, obtained using isentropic and isothermal operator splits. As expected, these Figures show that for strongly coupled problems (Case 2) the isothermal split leads to a completely unstable behavior ending with a blow-up of the solution, while the isentropic split provides the right solution. Despite this fact, for weakly coupled problems the two splits provide practically the same solution. This behavior has been shown in quasi-static and dynamic analyses, as well as for thermoelastic and thermoplastic constitutive responses.

4.2. Numerical simulations of solidification processes

(A) *Cylindrical aluminium solidification test.* This example, taken from CELENTANO, OLLER & OÑATE [1996], is concerned with the solidification process of a cylindrical aluminium specimen in a steel mould. The geometry of the problem is shown in FIGURE 4.6. Assumed starting conditions in the numerical simulation are given by a completely filled mould with aluminium in liquid state at a uniform temperature of 670°C. The initial temperature of the mould is 200°C. The material properties for the aluminium have been assumed to be temperature dependent, while constant material properties have been assumed for the steel mould. The external surfaces of the mould as well as the upper surface of the casting metal have been assumed perfectly insulated. A constant heat transfer coefficient $h_{co} = 10$ N/mm s °K and a gap dependent convection-radiation coefficient between the aluminium and the steel mould has been assumed. Only gravitational forces have been

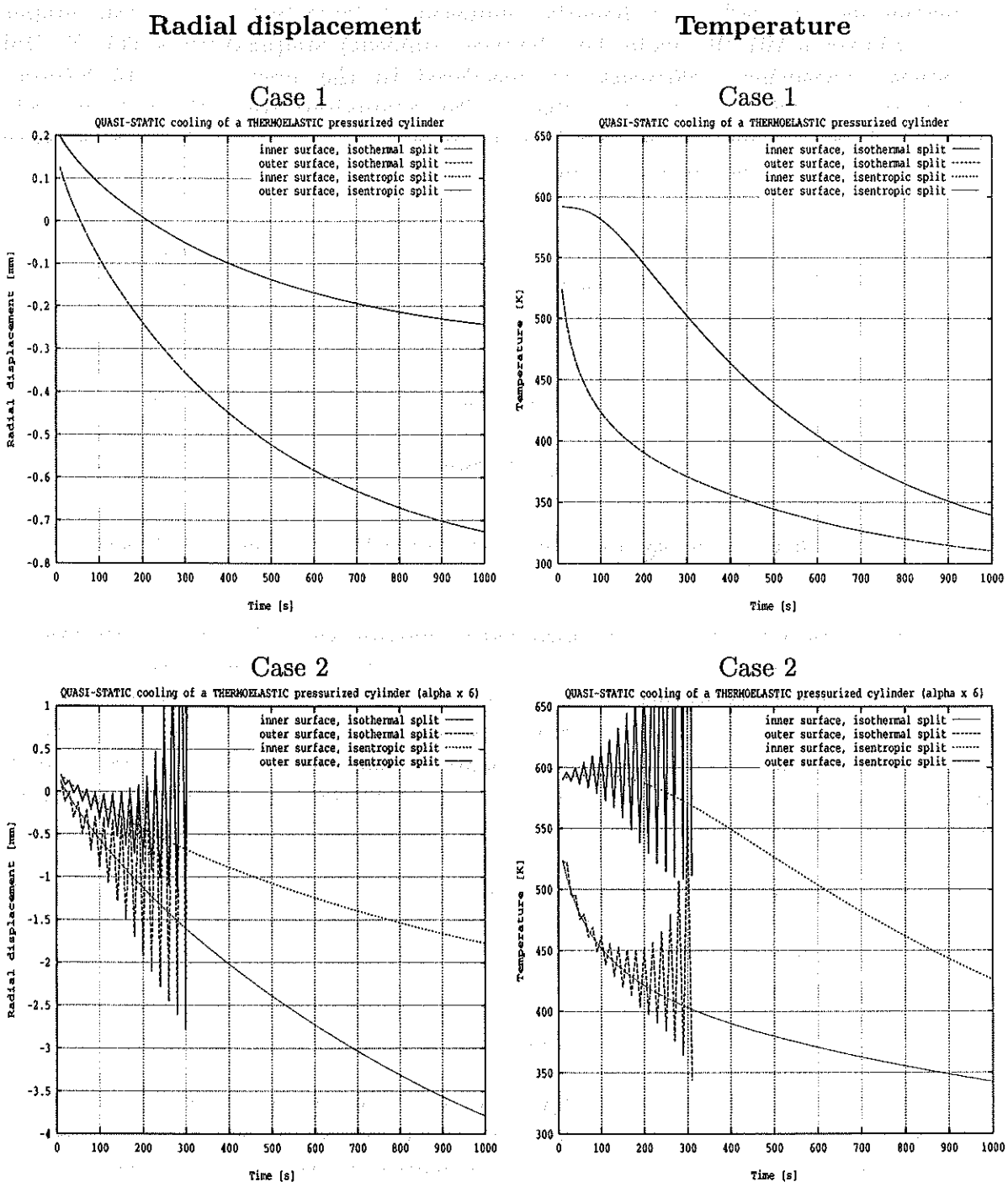

FIGURE 4.2. Quasi-static cooling of a thermoelastic pressurized thick-walled cylinder. Radial displacement and temperature at the inner and outer surfaces, using isentropic and isothermal operator splits, for a weakly coupled (Case 1) and strongly coupled (Case 2) cases.

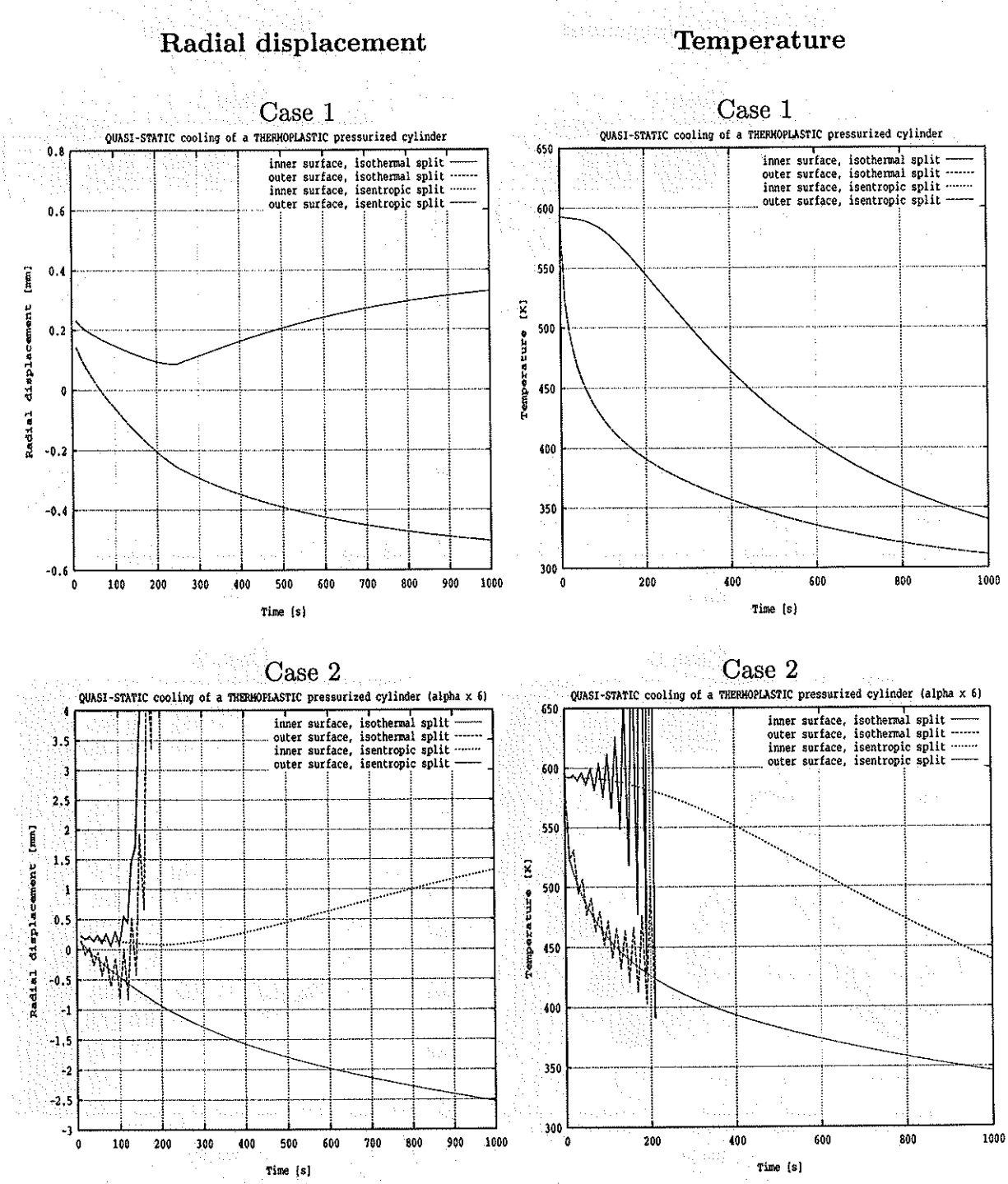

FIGURE 4.3. Quasi-static cooling of a thermoplastic pressurized thick-walled cylinder. Radial displacement and temperature at the inner and outer surfaces, using isentropic and isothermal operator splits, for a weakly coupled (Case 1) and strongly coupled (Case 2) cases.

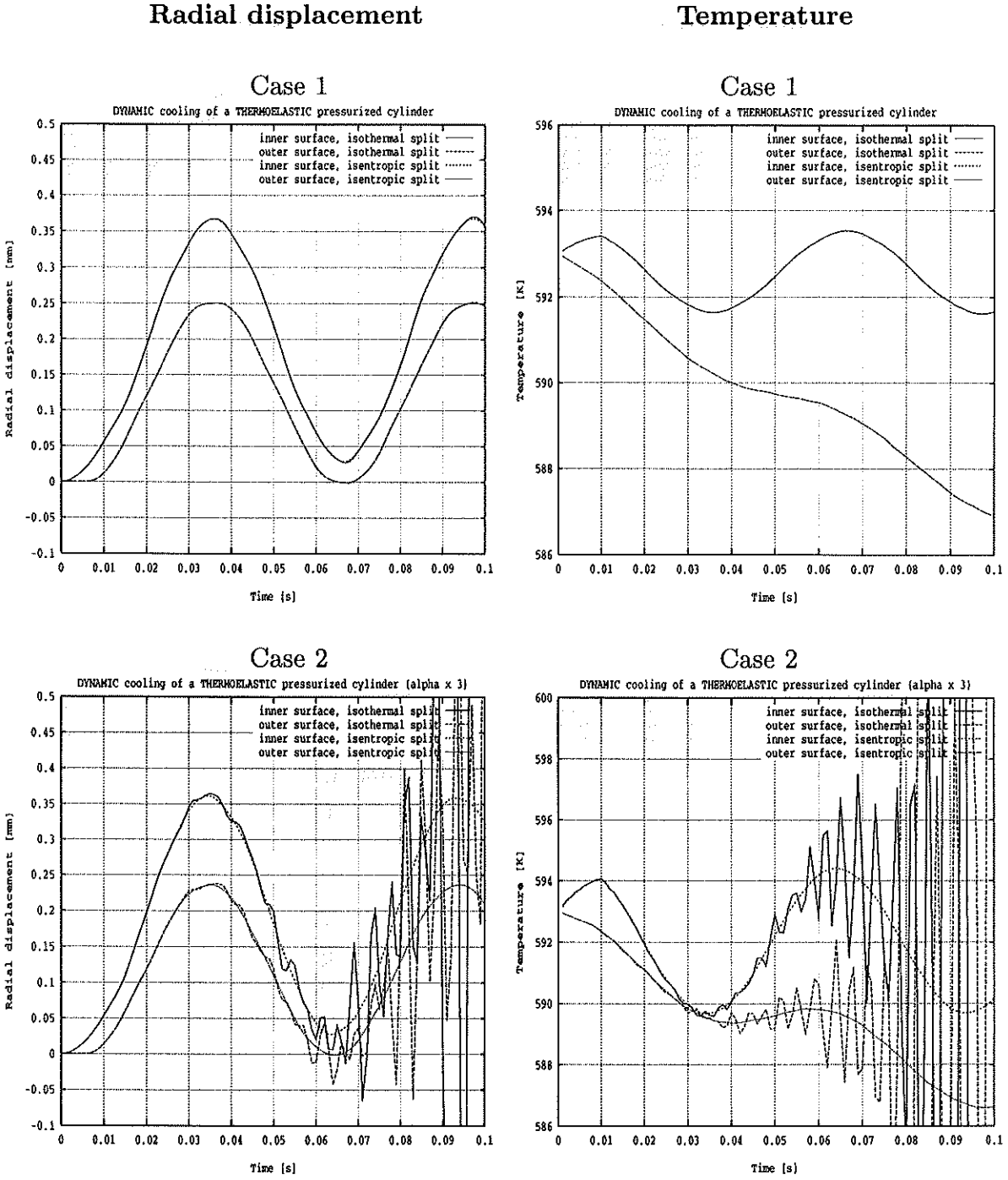

FIGURE 4.4. Dynamic cooling of a thermoelastic pressurized thick-walled cylinder. Radial displacement and temperature at the inner and outer surfaces, using isentropic and isothermal operator splits, for a weakly coupled (Case 1) and strongly coupled (Case 2) cases.

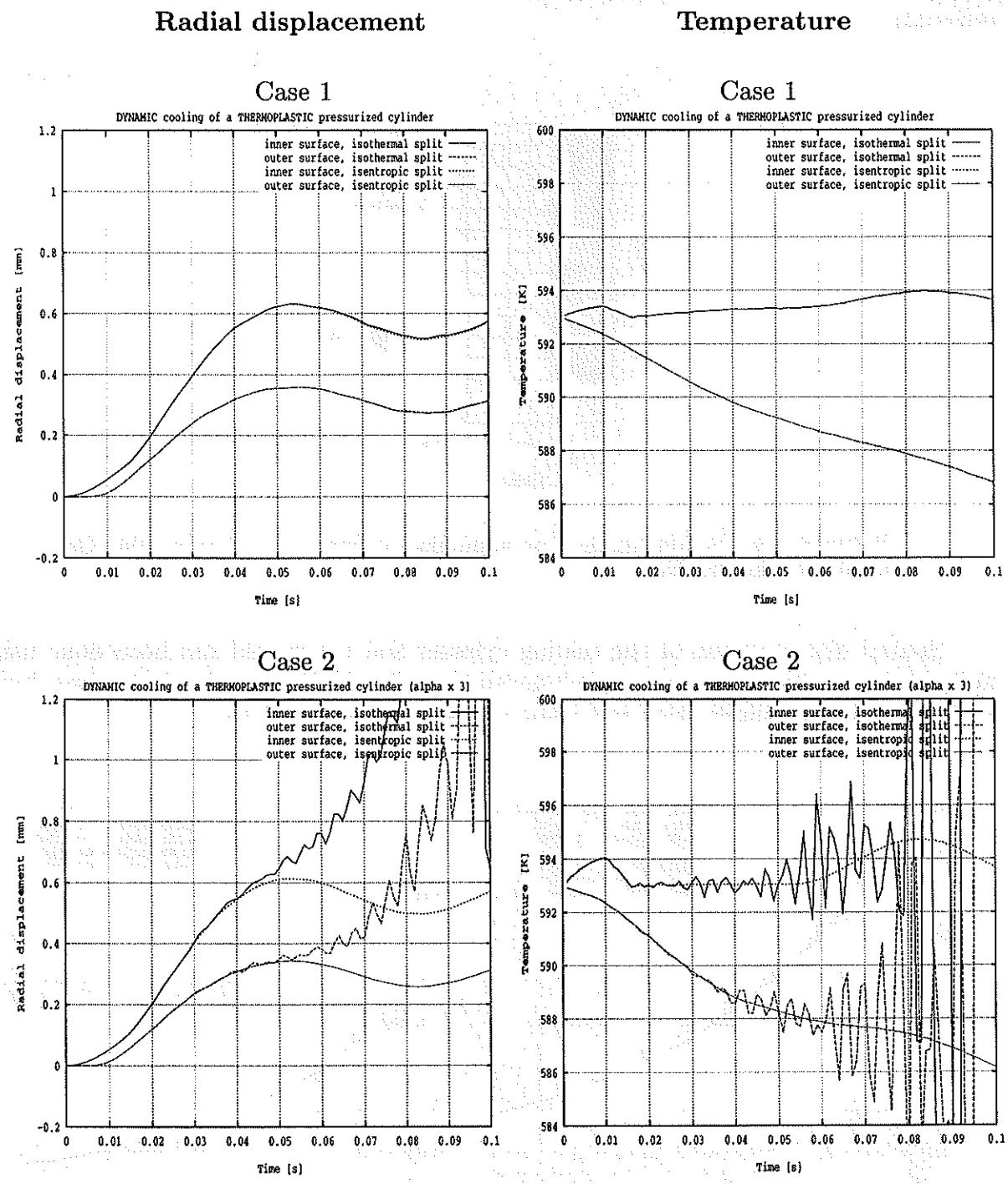

FIGURE 4.5. Dynamic cooling of a thermoplastic pressurized thick-walled cylinder. Radial displacement and temperature at the inner and outer surfaces, using isentropic and isothermal operator splits, for a weakly coupled (Case 1) and strongly coupled (Case 2) cases.

assumed. Further details on the geometrical and material data can be found in the above reference.

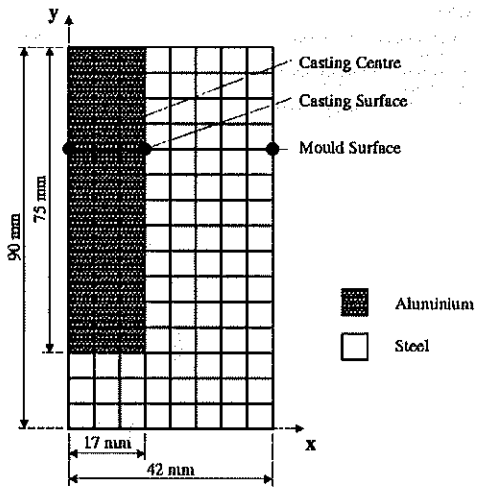

FIGURE 4.6. Solidification of an aluminium cylinder in a steel mould. Geometry of the problem.

Spatial discretization of the casting cylinder and the mould has been done using a finite element mesh of axisymmetric 3-noded triangles. Numerical simulation was done up to 90 secs. of the solidification test using a time increment of 1 sec.

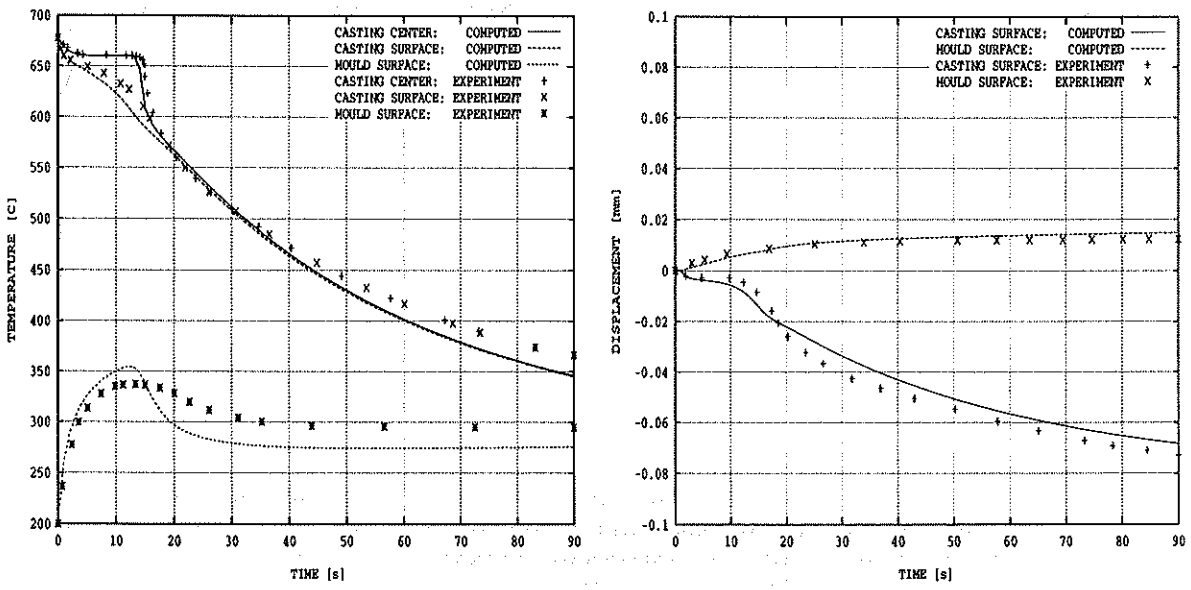

FIGURE 4.7. Solidification of an aluminium cylinder in a steel mould. (a) Temperature evolution at the casting center, casting surface and mould surface for an intermediate section. (b) Radial displacement evolution at the casting surface and mould surface for an intermediate section.

FIGURE 4.7A shows the temperature evolution at the casting center, casting surface and mould surface for an intermediate section. A typical temperature plateau due to the release of latent heat during solidification can be seen in the casting center point of this section up to 15 secs. approximately. FIGURE 4.7B shows the evolution of the radial displacements at the casting and mould surfaces for the same intermediate section. The difference between the two curves gives the gap distance evolution at the chosen section. Temperature and air gap evolution predicted by the model compare very well with experimental results. A data sensitivity analysis has shown a strong influence of the heat convection coefficient between aluminium and mould in the temperature evolution.

(B) *Solidification of a Renault Clio crankshaft.* This example deals with the numerical simulation of the solidification process of an industrial part, in this case, a Renault *Clio* crankshaft. Geometrical and material data, as well as experimental results, were provided by Renault. FIGURE 4.8 shows a view of the finite element mesh used for the part, consisting of nearly 15,000 4-noded tetrahedral elements. The sand mould has been discretized using around another 30,000 4-noded tetrahedral elements.

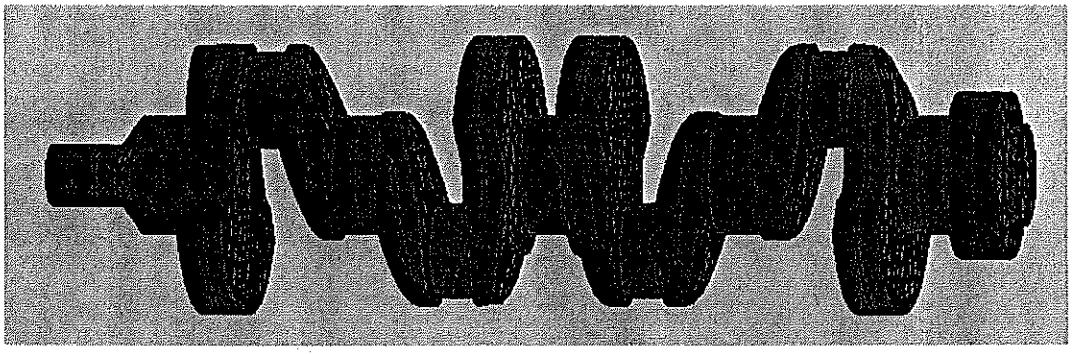

FIGURE 4.8. Solidification of a Renault *Clio* crankshaft. Finite element mesh of the part.

The temperature distribution at the part at different stages of the analysis, using a quarter section view, is shown in FIGURE 4.9. FIGURES 4.10 and 4.11 show the temperature distribution on sections x-y and x-z, respectively, of the deformed shape of the part. In these Figures it is also clearly shown the evolution of the gap between the part and the mould. The evolution of the mushy zone, given by the temperature evolution at the liquid-solid transition phase, is shown in FIGURE 4.12. A comparison between the computed and the experimental temperature evolution at different points is shown in FIGURES 4.13A and 4.13B, where a good agreement is observed.

5. CONCLUDING REMARKS

A formulation of coupled thermoplastic problems with phase-change has been presented. The formulation has been consistenly derived within a thermodynamic framework. A particular J2 thermoplastic model has been considered in which the material properties have been assumed to be temperature dependent. Operator splits of the governing differential equations, and their nonlinear stability properties, have been discussed. Within

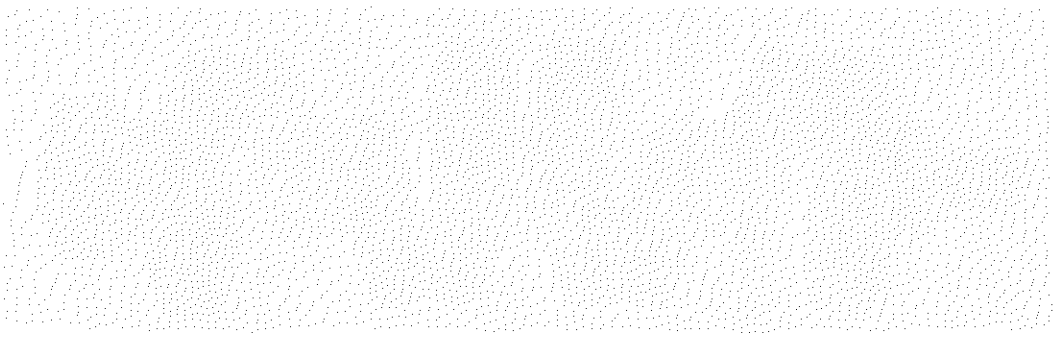

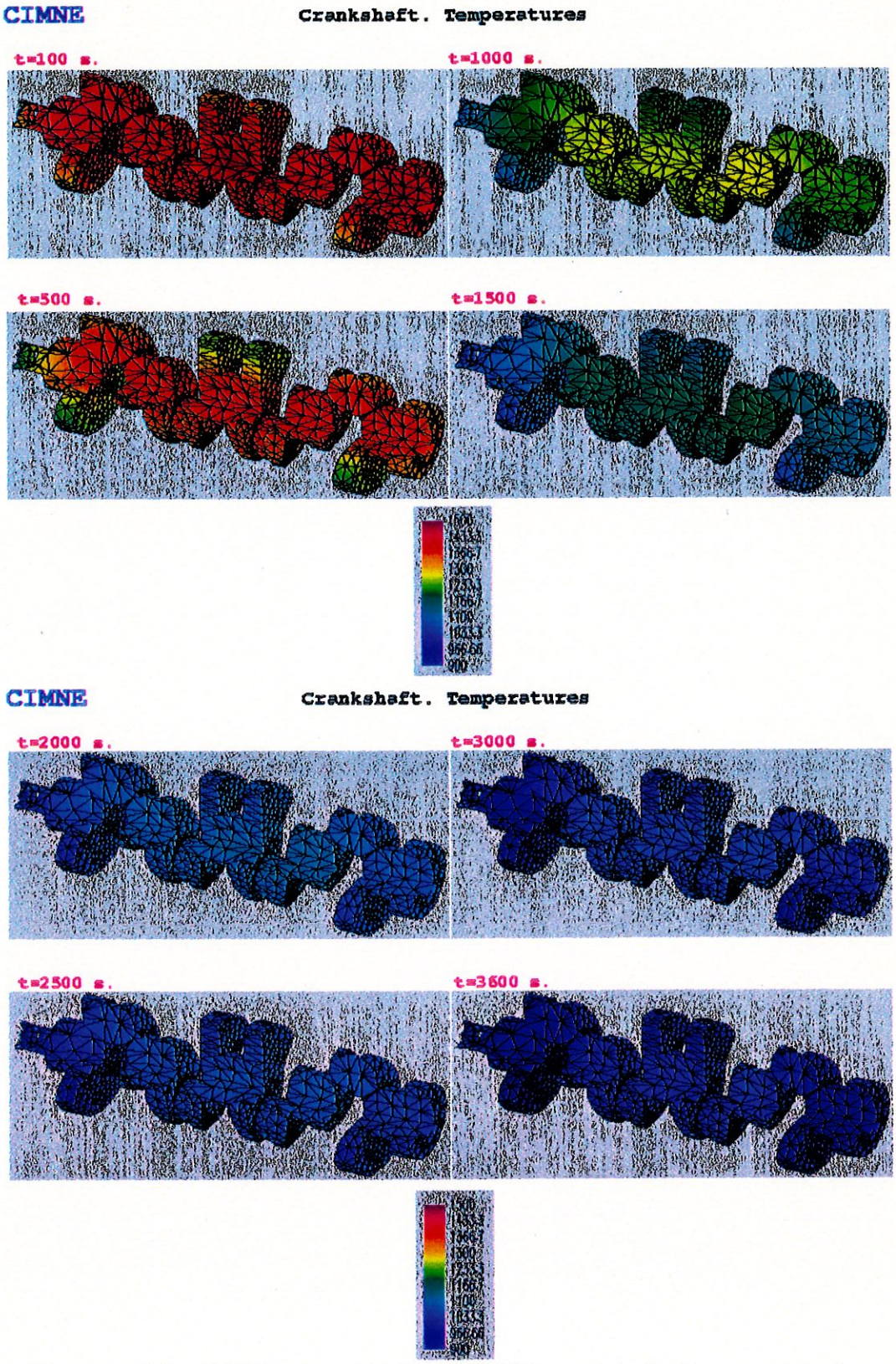

FIGURE 4.9. Solidification of a Renault *Clio* crankshaft. Temperature distribution at different stages of the solidification process.

Introduction

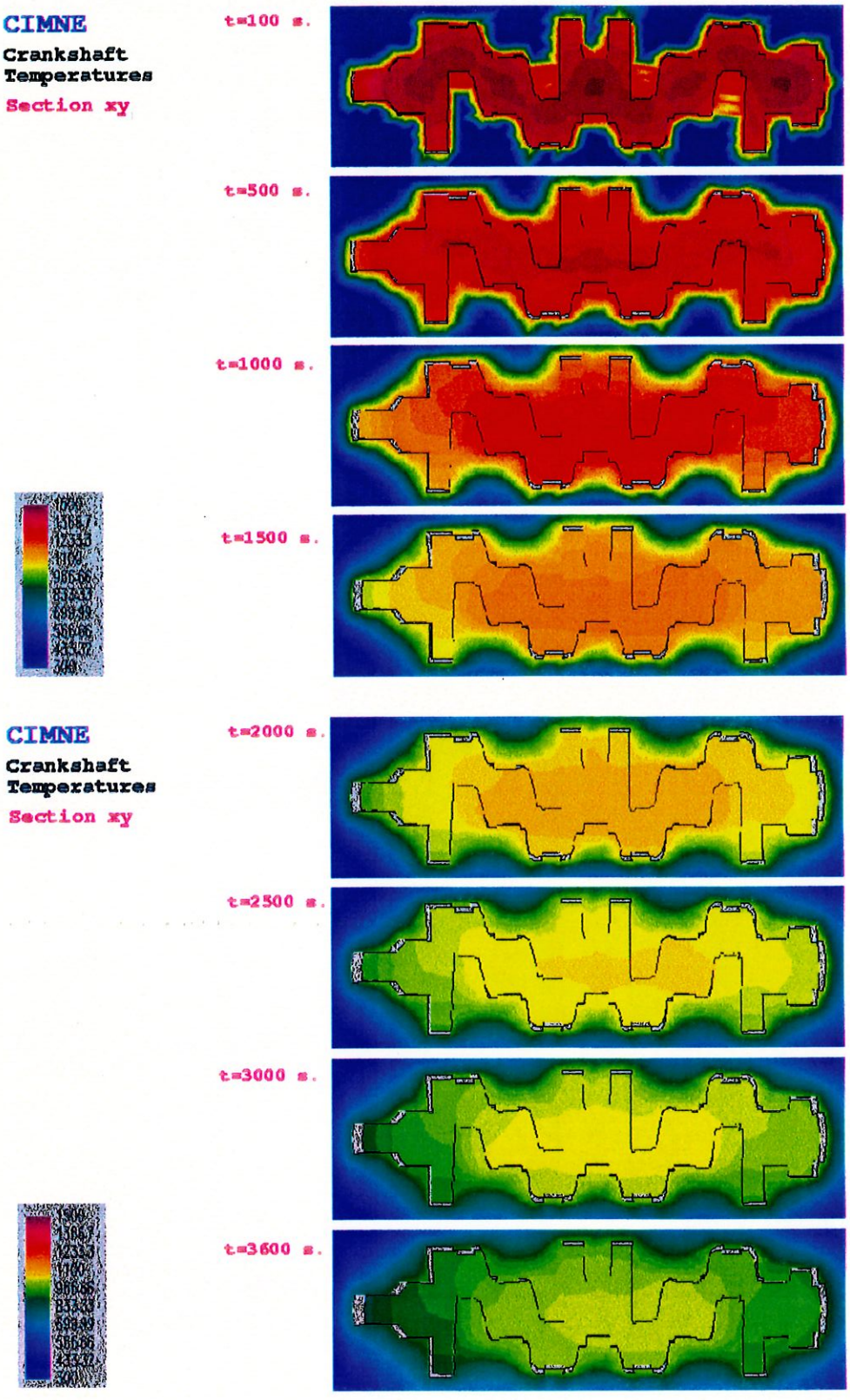

FIGURE 4.10. Solidification of a Renault *Clio* crankshaft. Temperature distribution at different stages of the solidification process. Section x-y.

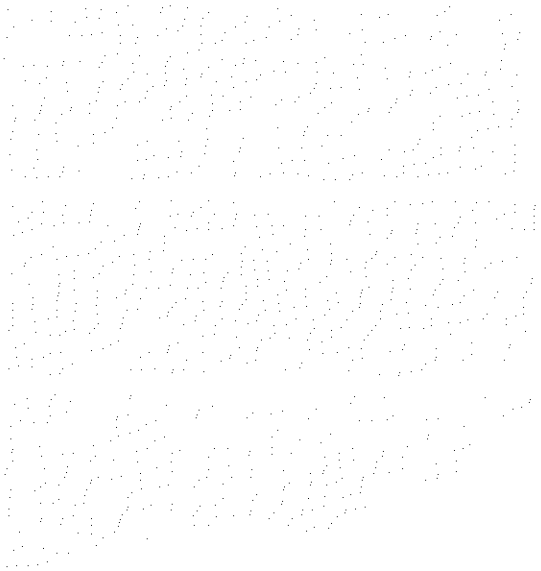

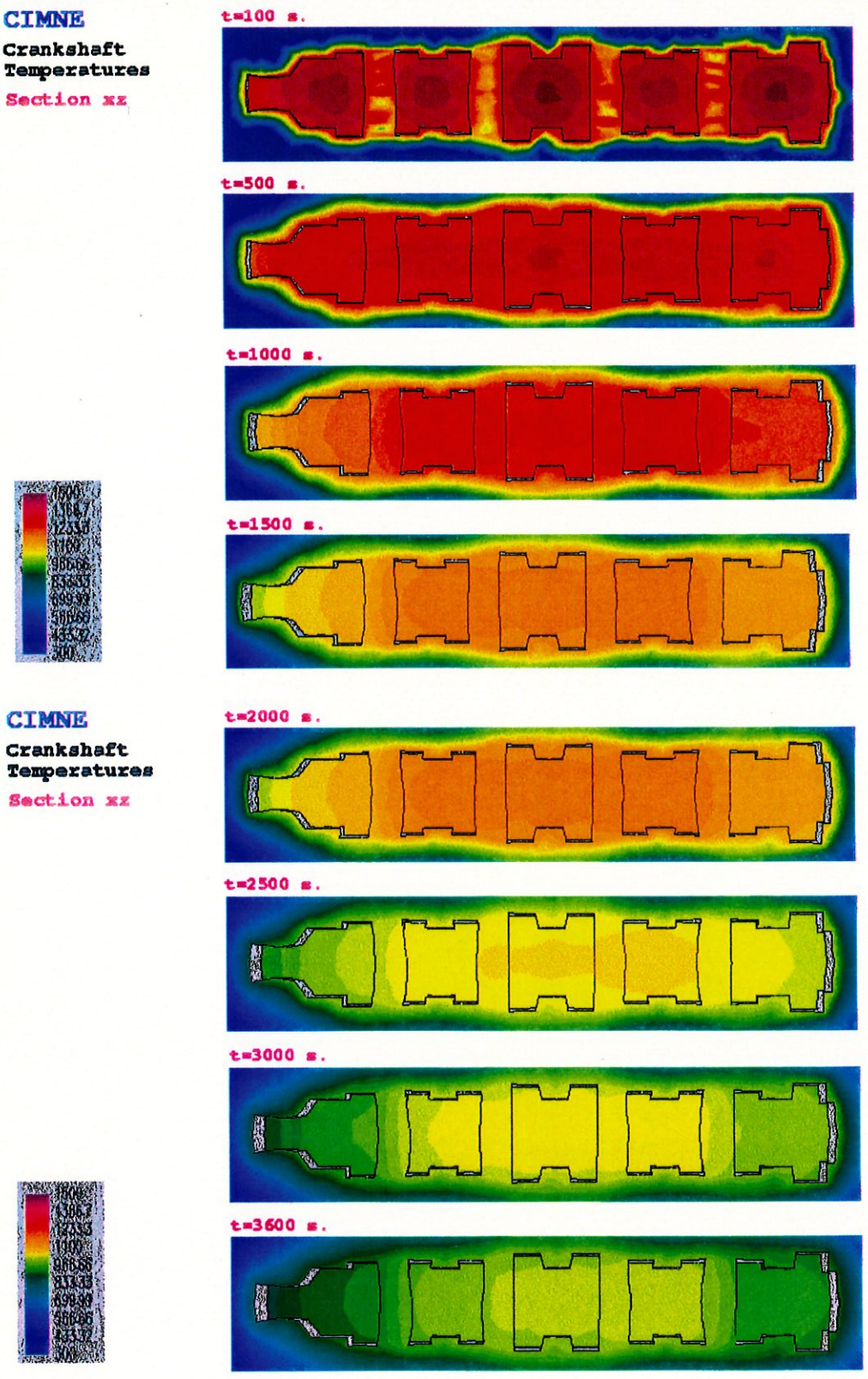

FIGURE 4.11. Solidification of a Renault *Clio* crankshaft. Temperature distribution at different stages of the solidification process. Section x-z.

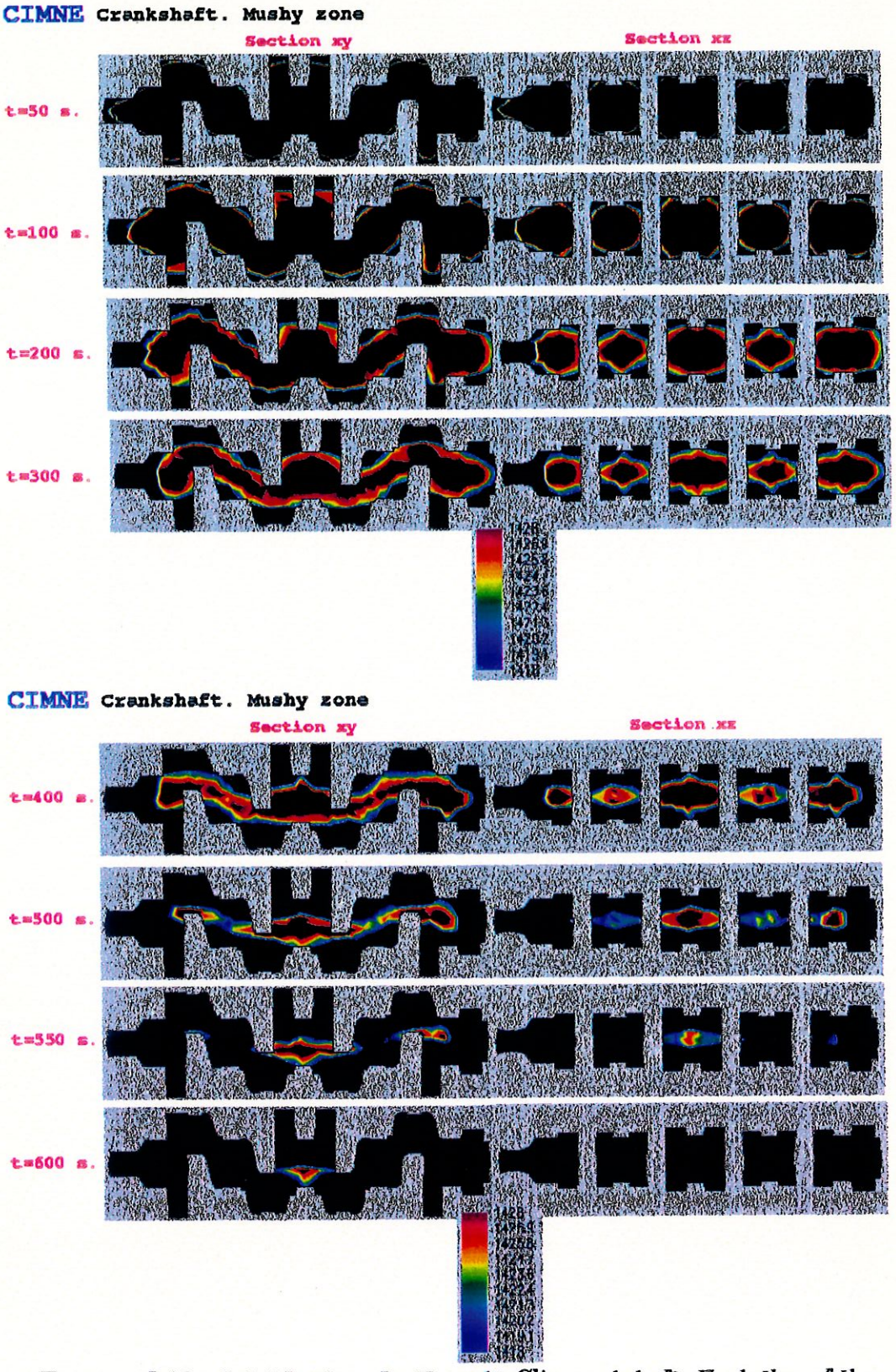

FIGURE 4.12. Solidification of a Renault *Clio* crankshaft. Evolution of the mushy zone. Temperature distribution at different stages of the solidification process. Sections x-y and x-z.

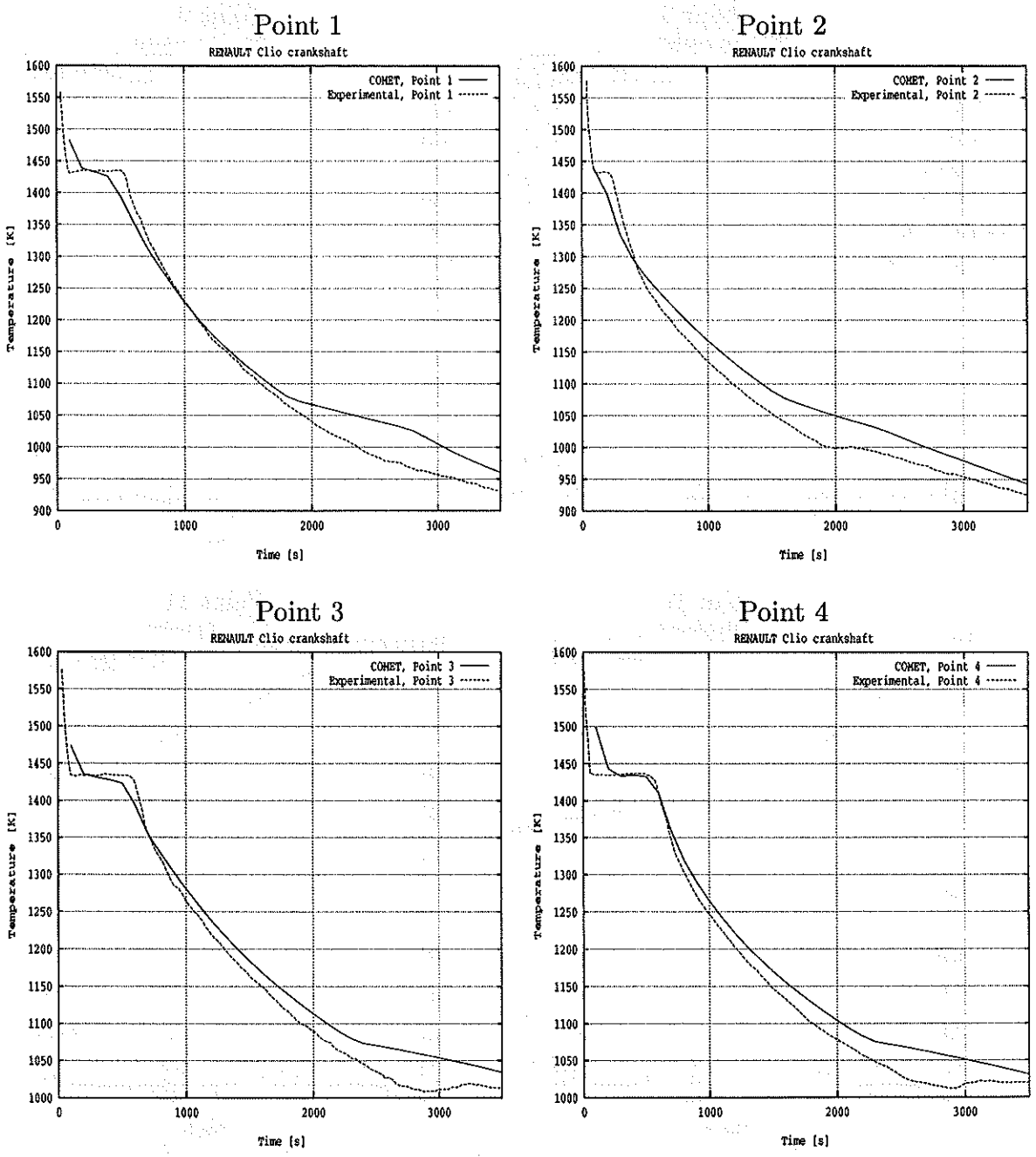

FIGURE 4.13A. Solidification of a Renault *Clio* crankshaft. Temperature evolution at different points.

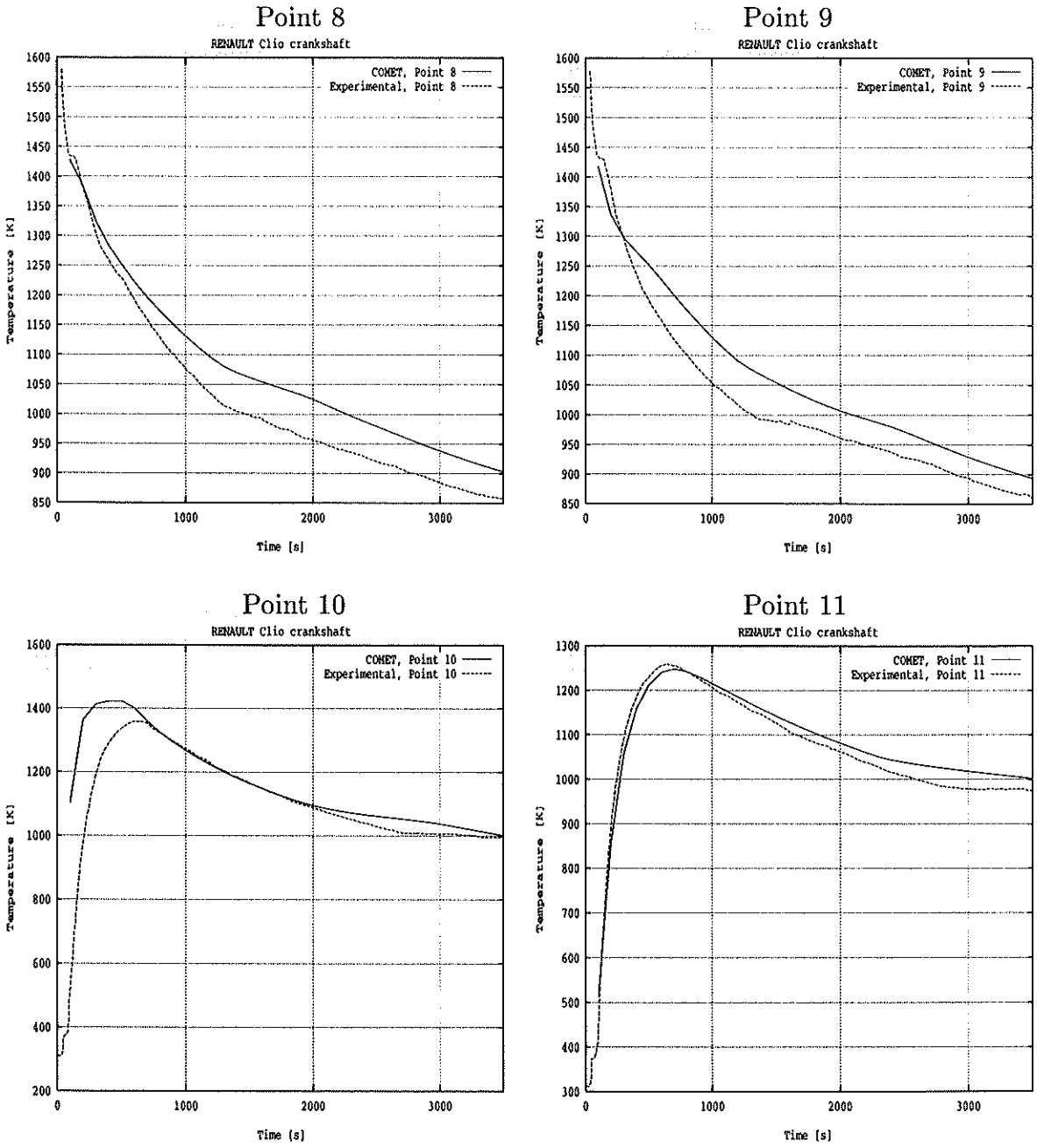

FIGURE 4.13B. Solidification of a Renault *Clio* crankshaft. Temperature evolution at different points.

the isentropic operator split, additional split design constraints have been introduced. A numerical assessment of the accuracy and nonlinear stability properties of the isentropic and isothermal splits has been performed. Numerical results obtained in the simulation of solidification processes show a good agreement with the experimental data available.

ACKNOWLEDGEMENTS

Financial support for this work has been provided by RENAULT under contract CIMNE/1997/001-Affectation:H5.21.41 with CIMNE. This support is gratefully acknowledged.

REFERENCES

AGELET DE SARACIBAR, C. [1997A], "A New Frictional Time Integration Algorithm for Multi-Body Large Slip Frictional Contact Problems", *Computer Methods in Applied Mechanics and Engineering*, **142**, 303-334.

AGELET DE SARACIBAR, C. [1997B], "Numerical Analysis of Coupled Thermomechanical Contact Problems. Computational Model and Applications", *Archives of Computational Methods in Engineering*, to be published.

ARMERO, F. & J.C. SIMO [1992A], "A new Unconditionally Stable Fractional Step Method for Nonlinear Coupled Thermomechanical Problems", *International Journal for Numerical Methods in Engineering*, **35**, 737-766.

ARMERO F. & J.C. SIMO [1992B], "Product Formula Algorithms for Nonlinear Coupled Thermoplasticity: Formulation and Nonlinear Stability Analysis", *Division of Applied Mechanics, Department of Mechanical Engineering, Stanford University, Stanford, California*, SUDAM Report no. 92-4, March 1992.

ARMERO F. & J.C. SIMO [1993], "A Priori Stability Estimates and Unconditionally Stable Product Algorithms for Nonlinear Coupled Thermoplasticity", *International Journal of Plasticity*, **9**, 749-782.

LAURSEN, T.A. [1992], "Formulation and Treatment of Frictional Contact Problems Using Finite Elements", *Ph.D. Dissertation*, Stanford University, Division of Applied Mechanics, Report no. 92-6.

LAURSEN, T.A. & S. GOVINDJEE [1994], "A Note on the Treatment of Frictionless Contact Between Non-smooth Surfaces in Fully Non-linear Problems", *Communications in Applied Numerical Methods*, **10**, 869-878

LAURSEN, T.A. & J.C. SIMO [1991], "On the Formulation and Numerical Treatment of Finite Deformation Frictional Contact Problems", in *Nonlinear Computational Mechanics–State of the Art*, P. Wriggers & W. Wagner, eds., Springer-Verlag, Berlin, pp. 716-736.

LAURSEN, T.A. & J.C. SIMO [1992], "Formulation and Regularization of Frictional Contact Problems for Lagrangian Finite Element Computations", in *Proc. of The Third International Conference on Computational Plasticity: Fundamentals and Applications, COMPLAS III*, D.R.J. Owen, E. Oñate & E. Hinton, eds., Pineridge Press, Swansea, pp. 395-407.

LAURSEN, T.A. & J.C. SIMO [1993A], "A Continuum-Based Finite Element Formulation for the Implicit Solution of Multi-Body, Large Deformation Frictional Contact Problems", *International Journal for Numerical Methods in Engineering*, **36**(20), 3451-3485.

LAURSEN, T.A. & J.C. SIMO [1993B], "Algorithmic Symmetrization of Coulomb Frictional Problems Using Augmented Lagrangians", *Computer Methods in Applied Mechanics and Engineering*, **108**, 133-146.

SIMO, J.C. [1994], "Numerical Analysis Aspects of Plasticity", in *Handbook of Numerical Analysis, Volume IV*, P.G. Ciarlet and J.J. Lions, eds., Nort-Holland.

SIMO, J.C. & F. ARMERO [1991], "Recent Advances in the Formulation and Numerical Analysis of Thermoplasticity at Finite Strains", in *Finite Inelastic Deformations - Theory and Applications*, E. Stein and D. Besdo, eds., IUTAM/IACM Symposium, Hannover, FRG, August, 19-23, 1991 Springer-Verlag, Berlin, 1991.

SIMO, J.C. & C. MIEHE [1992], "Associative Coupled Thermoplasticity at Finite Strains: Formulation, Numerical Analysis and Implementation", *Computer Methods in Applied Mechanics and Engineeering*, **98**, 41-104.

WRIGGERS, P. & C. MIEHE [1992], "Recent Advances in the Simulation of Thermomechanical Contact Processes", in *Proc. of The Third International Conference on Computational Plasticity: Fundamentals and Applications, COMPLAS III*, D.R.J. Owen, E. Oñate & E. Hinton, eds., Pineridge Press, Swansea, pp. 325-347.

WRIGGERS, P. & C. MIEHE [1994], "Contact Constraints within Coupled Thermomechanical Analysis. A Finite Element Model", *Computer Methods in Applied Mechanics and Engineering*, **113**, 301-319.

WRIGGERS, P. & G. ZAVARISE [1993], "Thermomechanical Contact. A Rigorous but Simple Numerical Approach", *Computers and Structures*, **46**, 47-53.

CELENTANO, D., S. OLLER & E. OÑATE [1996], "A Coupled Thermomechanical Model for the Solidification of Cast Metals", *Int. J. Solids Struct.*, **33** (5), 647-673.

APPENDIX I. RETURN MAPPING ALGORITHMS

In this appendix we summarize the main steps involved in the return mapping algorithms for the mechanical and thermal problems arising from the isentropic operator split. Note that for the mechanical problem an isentropic return mapping algorithm is performed, while for the thermal problem the classical isothermal return mapping is performed.

I.A. Mechanical problem

i. Step 1. *Trial state (kinematics).*
Given the initial data $\{\epsilon_n, \Theta_n\}$ and database $\{\epsilon_n^p, \xi_n\}$ at time t_n and prescribed ϵ_{n+1} at time t_{n+1}, set:

$$\begin{aligned} \epsilon_{n+1}^{p\ trial} &:= \epsilon_n^p, \\ \xi_{n+1}^{trial} &:= \xi_n, \\ \epsilon_{n+1}^{e\ trial} &:= \epsilon_{n+1} - \epsilon_{n+1}^{p\ trial}. \end{aligned}$$

ii. Step 2. *Trial temperature.*
IF (constant material properties) THEN

$$\Theta_{n+1}^{trial} := \hat{\Theta}(e_{n+1}, H_n^e, \xi_{n+1}^{trial}) \ \text{ with}$$
$$e_{n+1} := \mathrm{tr}[\epsilon_{n+1}] \ \text{ and } \ H_n^e := \hat{H}^e(e_n, \Theta_n, \xi_n),$$

ELSE

Solve for Θ_{n+1}^{trial} the implicit nonlinear equation:

$$\hat{H}^e(e_{n+1}, \Theta_{n+1}^{trial}, \xi_{n+1}^{trial}) - H_n^e = 0.$$

END IF

iii. Step 3. *Trial (generalized) stresses.*

$$\begin{aligned} \boldsymbol{s}_{n+1}^{trial} &:= \mathrm{dev}[\boldsymbol{\sigma}_{n+1}^{trial}] = 2\mu_{n+1}^{trial}\mathrm{dev}[\epsilon_{n+1}^{e\ trial}], \\ p_{n+1}^{trial} &:= \kappa_{n+1}^{trial} e_{n+1} - 3\kappa_{n+1}^{trial}\alpha_{n+1}^{trial}(\Theta_{n+1}^{trial} - \Theta_0), \\ q_{n+1}^{trial} &:= -\hat{K}_\xi(\xi_{n+1}^{trial}, \Theta_{n+1}^{trial}). \end{aligned}$$

iv. Step 4. *Trial yield function.*

$$\Phi_{n+1}^{trial} := \hat{\Phi}(\boldsymbol{\sigma}_{n+1}^{trial}, q_{n+1}^{trial}, \Theta_n) = \|\boldsymbol{s}_{n+1}^{trial}\| - \sqrt{\frac{2}{3}}[y_0(\Theta_n) - q_{n+1}^{trial}]$$

IF $\Phi_{n+1}^{trial} \leq 0$ THEN

Set $(\cdot)_{n+1} := (\cdot)_{n+1}^{trial}$ and update database
RETURN

END IF

v. Step 5. *Isentropic return mapping.*

IF (constant material properties) THEN

Solve for γ_{n+1} the implicit nonlinear equation:

$$\Phi_{n+1} := \hat{\Phi}(\boldsymbol{\sigma}_{n+1}, q_{n+1}, \Theta_n) = 0 \quad \text{with}$$
$$\Theta_{n+1} = \hat{\Theta}(e_{n+1}, H^e_n, \xi_{n+1}),$$

ELSE

Solve for γ_{n+1} and Θ_{n+1} the implicit nonlinear set of equations:

$$\left.\begin{aligned} \Phi_{n+1} &:= \hat{\Phi}(\boldsymbol{\sigma}_{n+1}, q_{n+1}, \Theta_n) = 0, \\ \hat{H}^e(e_{n+1}, \Theta_{n+1}, \xi_{n+1}) - H^e_n &= 0, \end{aligned}\right\}$$

END IF

$$\Phi_{n+1} := \|\boldsymbol{s}^{trial}_{n+1}\| \frac{\mu_{n+1}}{\mu^{trial}_{n+1}} - 2\mu_{n+1}\gamma_{n+1} - \sqrt{\frac{2}{3}}[y_0(\Theta_n) - q_{n+1}],$$
$$\xi_{n+1} = \xi^{trial}_{n+1} + \sqrt{\frac{2}{3}}\gamma_{n+1},$$
$$q_{n+1} = -\hat{K}_\xi(\xi_{n+1}, \Theta_{n+1}).$$

vi. Step 6. *Update database and compute stresses.*

$$\boldsymbol{\epsilon}^p_{n+1} = \boldsymbol{\epsilon}^{p\ trial}_{n+1} + \gamma_{n+1}\boldsymbol{n}^{trial}_{n+1},$$
$$\boldsymbol{s}_{n+1} = \boldsymbol{s}^{trial}_{n+1}\frac{\mu_{n+1}}{\mu^{trial}_{n+1}} - 2\mu_{n+1}\gamma_{n+1}\boldsymbol{n}^{trial}_{n+1},$$
$$p_{n+1} = \kappa_{n+1}e_{n+1} - 3\kappa_{n+1}\alpha_{n+1}(\Theta_{n+1} - \Theta_0),$$
$$\boldsymbol{\sigma}_{n+1} = p_{n+1}\,\mathbf{1}_3 + \boldsymbol{s}_{n+1},$$

where

$$\boldsymbol{n}^{trial}_{n+1} := \boldsymbol{s}^{trial}_{n+1}/\|\boldsymbol{s}^{trial}_{n+1}\|.$$

I.B. Thermal problem

i. Step 1. *Trial state (kinematics).*

Given the initial data $\{\boldsymbol{\epsilon}_n, \Theta_n\}$ and database $\{\boldsymbol{\epsilon}^p_n, \xi_n\}$ at time t_n and prescribed $\{\boldsymbol{\epsilon}_{n+1}, \Theta_{n+1}\}$ at time t_{n+1}, set:

$$\boldsymbol{\epsilon}^{p\ trial}_{n+1} := \boldsymbol{\epsilon}^p_n,$$
$$\xi^{trial}_{n+1} := \xi_n,$$
$$\boldsymbol{\epsilon}^{e\ trial}_{n+1} := \boldsymbol{\epsilon}_{n+1} - \boldsymbol{\epsilon}^{p\ trial}_{n+1}.$$

ii. Step 2. *Trial (generalized) stresses.*

$$\boldsymbol{s}_{n+1}^{trial} := \mathrm{dev}[\boldsymbol{\sigma}_{n+1}^{trial}] = 2\mu_{n+1}\mathrm{dev}[\boldsymbol{\epsilon}_{n+1}^{e\ trial}],$$
$$q_{n+1}^{trial} := -K_\xi(\xi_{n+1}^{trial}, \Theta_{n+1}).$$

iii. Step 3. *Trial yield function.*

$$\Phi_{n+1}^{trial} := \hat{\Phi}(\boldsymbol{\sigma}_{n+1}^{trial}, q_{n+1}^{trial}, \Theta_{n+1})$$
$$= \|\boldsymbol{s}_{n+1}^{trial}\| - \sqrt{\frac{2}{3}}[y_0(\Theta_{n+1}) - q_{n+1}^{trial}]$$

IF $\Phi_{n+1}^{trial} \leq 0$ THEN

Set $(\cdot)_{n+1} := (\cdot)_{n+1}^{trial}$ and update database
RETURN

END IF

iv. Step 4. *Isothermal return mapping.*
Solve for γ_{n+1} the implicit nonlinear equation:

$$\Phi_{n+1} := \hat{\Phi}(\boldsymbol{\sigma}_{n+1}, q_{n+1}, \Theta_{n+1}) = 0 \quad \text{with}$$
$$\Phi_{n+1} := \|\boldsymbol{s}_{n+1}^{trial}\| - 2\mu_{n+1}\gamma_{n+1} - \sqrt{\frac{2}{3}}[y_0(\Theta_{n+1}) - q_{n+1}],$$
$$\xi_{n+1} = \xi_{n+1}^{trial} + \sqrt{\frac{2}{3}}\gamma_{n+1},$$
$$q_{n+1} = -\hat{K}_\xi(\xi_{n+1}, \Theta_{n+1}).$$

v. Step 5. *Update database.*

$$\boldsymbol{\epsilon}_{n+1}^{p} = \boldsymbol{\epsilon}_{n+1}^{p\ trial} + \gamma_{n+1}\boldsymbol{n}_{n+1}^{trial},$$

where

$$\boldsymbol{n}_{n+1}^{trial} := \boldsymbol{s}_{n+1}^{trial}/\|\boldsymbol{s}_{n+1}^{trial}\|.$$

vi. Step 6. *Plastic mechanical dissipation.*

$$\mathcal{D}_{mech\,n+1} = \sqrt{\frac{2}{3}}\gamma_{n+1}\ y_0(\Theta_{n+1})/\Delta t.$$

List of Figures

FIGURE 4.13A. Solidification of a Renault *Clio* crankshaft. Temperature evolution at different points.

FIGURE 4.13B. Solidification of a Renault *Clio* crankshaft. Temperature evolution at different points.